



Graduate Theses, Dissertations, and Problem Reports

2006

A PC-based fluid and heat transfer analyzer for two-phase flow in pipes

Gbolahan Afonja
West Virginia University

Follow this and additional works at: <https://researchrepository.wvu.edu/etd>

Recommended Citation

Afonja, Gbolahan, "A PC-based fluid and heat transfer analyzer for two-phase flow in pipes" (2006). *Graduate Theses, Dissertations, and Problem Reports*. 3241.
<https://researchrepository.wvu.edu/etd/3241>

This Thesis is protected by copyright and/or related rights. It has been brought to you by the The Research Repository @ WVU with permission from the rights-holder(s). You are free to use this Thesis in any way that is permitted by the copyright and related rights legislation that applies to your use. For other uses you must obtain permission from the rights-holder(s) directly, unless additional rights are indicated by a Creative Commons license in the record and/ or on the work itself. This Thesis has been accepted for inclusion in WVU Graduate Theses, Dissertations, and Problem Reports collection by an authorized administrator of The Research Repository @ WVU. For more information, please contact researchrepository@mail.wvu.edu.

A PC-Based Fluid and Heat Transfer Analyzer for Two-Phase Flow in Pipes

Gbolahan Afonja

Thesis submitted to the
College of Engineering and Mineral Resources
at West Virginia University
in partial fulfillment of the requirements
for the degree of

Master of Science
in
Petroleum & Natural Gas Engineering

Ilkin Bilgesu, Ph.D., Chair
Sam Ameri, M.S.
Daniel Della-Giustina, Ph.D.

Department of Petroleum and Natural Gas Engineering

Morgantown, West Virginia

2006

Keywords: Fluid Flow, Pipe Flow, Heat Transfer, Pressure Drop, Pressure Gradient

Abstract

A PC-Based Fluid and Heat Transfer Analyzer for Two-Phase Flow in Pipes

Gbolahan Afonja

Modeling the simultaneous flow of gas and liquid or two-phase gas-liquid flow in pipes is a key aspect in petroleum production. These models can enhance our ability to estimate fluid properties, predict pressure loss, liquid holdup, and flow pattern, and to see the effects of introducing concepts such as heat transfer to the system. Modeling two-phase flow phenomenon also allows visualization of the interaction of one property or parameter to another. The understanding of heat transfer in two-phase gas-liquid flow is important for economic and optimized operations.

This work focuses on the design of a PC-Based Software for modeling the effect of convective heat transfer on flow patterns in two-phase gas-liquid flow in pipes at all inclinations from -90° to $+90^\circ$ from horizontal, with the utilization of a temperature and pressure traverse along the length of the pipe. The implementation of this model in a computer program involves substantial calculations and correlations, some of which require iterative procedures.

Acknowledgements

I would like to express my appreciation and gratitude to my academic advisor, Dr. Ilkin Bilgesu. His understanding, patience, assistance, and friendly approach has helped me to go through my hard times during my studies.

I would also like to thank Dr. Shahab Mohaghegh, Dr. Kashy Aminian, and Dr. Razi Gaskari for their guidance and supervision through my work here at West Virginia University. I am also very thankful to my examining committee members, Professor Sam Ameri and Dr. Daniel Della-Giustina.

My appreciation also goes out to my fellow students and friends; Upender Nunsavathu, Peter Fadesere, Venkatta Kristamsetty, Sunil Lakshminarayanan, Allen Nfonsam, Michael Enoch, Raymond Sama, and Najeem Adeleke.

I wish to express my gratitude to Dr. Warren Myers of the College of Engineering, the Office of Social Justice, and the Petroleum and Natural Gas Engineering Department for providing financial support for my graduate studies.

Table of Contents

Abstract	ii
Acknowledgements	iii
Table of Contents	iv
List of Figures	vi
List of Tables	viii
Chapter 1 Introduction	1
1.1 Overview	1
1.2 Problem Statement	3
Chapter 2 Literature Review.....	4
2.1 Mechanistic Approach	4
2.2 Empirical Approach	5
Chapter 3 Theory.....	7
3.1 Two Phase Gas-Liquid Flow.....	7
3.1.1 Velocities and Flow rates.....	7
3.1.2 Flow Patterns.....	8
3.1.3 Flow Pattern Maps.....	11
3.1.4 Pressure Gradient	12
3.1.5 Holdup.....	13
3.1.6 Heat Transfer	13
3.2 Heat Transfer in Two-Phase Flow.....	17
3.2.1 Two-Phase Flow Correlations	17
3.2.1.1 Beggs and Brill Correlation.....	18

3.2.1.2	Mukherjee and Brill Correlation.....	24
3.2.2	Pressure Traverse.....	33
3.2.3	Heat Transfer	34
Chapter 4	Methodology	41
4.1	The Graphical User Interface	43
4.2	Relationships between results obtained.....	52
4.2.1	Angles, holdup and pressure gradient.....	52
4.2.2	Heat Transfer and Flow Pattern.....	55
4.2.3	Comparison with PipeSim.....	56
4.3	Sensitivity Runs	59
Chapter 5	Conclusions and Recommendations.....	71
5.1	Conclusions	71
5.2	Recommendations	72
References	73
Appendix	77
A.	Nomenclature	77
B.	Basic Oil and Gas Properties	79
B.1	Gas Properties	79
B.2	Oil Properties	86

List of Figures

Figure 3-1 Flow Patterns in Vertical and inclined flow (Wang et al, 2004)	9
Figure 3-2 Flow Patterns in horizontal and inclined flow (Wang et al, 2004)	10
Figure 3-3 Experimental Flow Pattern Map for air-water system in a horizontal pipe (Mandhane, 1974).....	11
Figure 3-4 Mechanistic Flow Pattern Map for air-water system in a slightly downward pipe (Taitel et al, 1976).....	12
Figure 3-5 Heat transfer setup for a pipe flow.	14
Figure 3-6 Flow chart for the prediction of Mukherjee and Brill Flow Pattern (Brill and Mukherjee, 1999).....	28
Figure 3-7 Control Volume for Stratified Flow.....	31
Figure 3-8 Temperature control volume in annular/stratified flow	37
Figure 4-1 Flowchart showing the program setup	42
Figure 4-2 Gas composition option	44
Figure 4-3 Window to input gas composition data.....	44
Figure 4-4 Gas specific gravity for empirical correlation	45
Figure 4-5 Oil and Gas Properties window.....	46
Figure 4-6 Fluid Dynamics window	47
Figure 4-7 Window showing pressure and temperature iteration, hydrodynamics, and thermal properties based on pipe length	48
Figure 4-8 Variation of temperature gradient ($^{\circ}\text{F}/\text{ft}$) with pipe length (ft).....	49
Figure 4-9 Iteration results.....	50
Figure 4-10 Key values	51

Figure 4-11 Variation of pressure gradient with pipe inclination angle	52
Figure 4-12 Variation of holdup with pipe angle	53
Figure 4-13 Mukherjee & Brill and Beggs & Brill (Pressure Gradient) against pipe angle	54
Figure 4-14 Beggs & Brill and Mukherjee & Brill (Holdup) against pipe angle.....	54
Figure 4-15 Relationship between overall coefficient of heat transfer (U) and convective coefficient of heat transfer (h) for bubble flow	55
Figure 4-16 Variation of pressure along pipe length for PipeSim and FHTA.....	58
Figure 4-17 Variation of temperature along pipe length for PipeSim and FHTA	59
Figure 4-18 Variation of pressure with pipe length for various reservoir temperatures	61
Figure 4-19 Variation of temperature gradient with pipe length for various reservoir temperatures.....	62
Figure 4-20 Variation of liquid holdup with pipe length for various reservoir temperatures.	63
Figure 4-21 Variation of pressure with pipe length at various GORs for horizontal flow.....	64
Figure 4-22 Variation of pressure with pipe length at various GORs for vertical flow	65
Figure 4-23 Pressure versus Liquid Holdup for Vertical and Horizontal flow.....	66
Figure 4-24 Variation of pressure with pipe length for horizontal Flow based on pipe ID...	67
Figure 4-25 Variation of pressure with pipe length for vertical flow based on pipe ID	68
Figure 4-26 Heat Transfer Coefficient for different pipe sizes	69
Figure 4-27 Holdup versus Pipe Length Based on Pipe ID for Vertical Flow.....	70

List of Tables

Table 3-1 Thermal Conductivities of materials	16
Table 3-2 Beggs and Brill empirical coefficients for H_L	20
Table 3-3 Beggs and Brill empirical coefficients for C.....	22
Table 3-4 Mukherjee and Brill Empirical Coefficients for H_L	27
Table 4-1 Example data for simulation.....	43
Table 4-2 Input values for comparison with PipeSim.....	57
Table 4-3 Input values for sensitivity runs.....	60

Chapter 1 Introduction

1.1 Overview

The flow of gas and liquids in pipes and the effect of thermal energy on the system are of importance in the chemical and petroleum industry. Flow assurance issues such as, paraffin deposition, hydrate formation, and heavy oil flow, which are crucial in the transportation of oil and gas through pipes, are related to the hydraulic and thermal factors of two-phase flow, thus the knowledge of heat transfer is vital in avoiding gas hydrate and deposition of wax resulting in repair, replacement, abandonment, or extra horsepower requirements (Kaminsky, 1999).

Some complexity exists in the modeling of gas-liquid flow because of the presence of gas and liquid phases. The interface between these two phases can occur in various geometrical distributions, and is mainly dependent on flow rates, physical properties of the fluids, and pipe inclination angles. This phenomenon is known as flow pattern. The thermal- and hydro-dynamics of the flow is heavily impacted from one flow pattern to another. For instance, some heat transfer parameters estimated using the stratified flow correlations might change by several orders of magnitude from those estimated by annular flow correlations (Chen, 2001).

Over the years, various mechanistic and empirical studies have been undertaken to calculate, predict, or model key factors in the hydrodynamics of two-phase flow, such as fluid properties, flow patterns, pressure drop, and liquid holdup; and thermal aspects such as heat transfer coefficient, overall heat transfer coefficient, and Nusselt number. The mechanistic method makes use of physical models, such as a high-pressure multiphase test facility

(Manabe et al, 2003) to predict hydrodynamics and heat transfer. The empirical method utilizes mathematical predictive models. Some studies have combined both the mechanistic and the empirical methods to give rise to the unified models.

1.2 Problem Statement

The purpose of this project is to develop a PC-Windows-Based Model for predicting two-phase gas-liquid pipe-flow phenomena such as flow patterns, pressure gradients, and the effect of flow pattern on convective heat transfer. The pipe inclination angle will also be considered, as this has been found to significantly affect flow geometry.

The system will calculate oil and gas property parameters from reservoir conditions, and use the results to estimate hydrodynamic factors, and heat transfer values.

Chapter 2 Literature Review

The complexity involved in modeling two-phase gas-liquid flow and its heat transfer has led to the emergence of various research works that seek to provide an understanding of these systems. Most of these studies can be grouped under three categories: mechanistic, correlative (empirical), and unified.

2.1 Mechanistic Approach

The mechanistic models take into consideration the physical mechanisms involved in the flow and heat processes. Investigators, with the acknowledgment that enhanced understanding of multiphase flow and heat transfer in pipes required a collective experimental and theoretical approach, made use of sophisticated test facilities that used instrumentation (such as high-speed cameras, nuclear densitometers, ultrasonics, and laser Doppler anemometers) for the measurement of crucial variables. Taitel et al (1976) and Dukler et al (1975) started the mechanistic modeling. Taitel et al (1976) identified four distinct flow patterns for upward two-phase flow. The flow patterns are bubble flow, slug flow, churn flow and annular flow. An improvement in mechanistic models is evident in the work to predict flow pattern for all inclination angles. Barnea (1986) pioneered a unified model that predicted flow geometry for a wide range of pipe inclination angles.

The works of Barnea, Taitel, and Dukler led to the enhancement of models that have been presented by Petalas and Aziz (1998), Xiao et al (1990), Ansari et al (1994), Gomez et al (2000), and Kaya et al (1999). These models contain the determination of flow patterns and the computation of pressure drop and hold up.

In the area of heat transfer, the mechanistic approach is a relatively recent development when compared to its application in fluid flow. The mechanistic approach for the prediction of heat transfer as it pertains to flow patterns consists of a flow pattern prediction model and a set of individual mechanistic models for predicting hydrodynamics and heat transfer. Manabe et al (2003) developed a heat transfer model for vertical two-phase flow. In their study, a high pressure multiphase test facility was used for experimental study, South Pelto crude oil (35° API gravity) was used as the liquid phase and natural gas supplied by Oklahoma Natural Gas Company was used as the gas phase. Ghajar and Kim (2005) studied the non-boiling two-phase flow heat transfer correlations for different flow patterns based on the pipe inclination angles.

2.2 Empirical Approach

Data obtained from laboratory test facilities, such as physical properties of gas and liquid, volumetric flow rates of the phases, inlet and outlet pipe pressures, pipe diameter and inclination angle, were used in the empirical approach. Sometimes field data was also incorporated in the system. The methods in this study fall under the empirical approach. Here, liquid holdup and pressure gradient are predicted for each flow pattern.

Beggs and Brill (1973) investigated gas-liquid flow to determine the effect of pipe inclination angle on liquid holdup and pressure loss in two-phase flow. They developed correlations for liquid holdup and friction factor which were used to predict pressure gradients for many flow conditions. In order to overcome some of the limitations of the Beggs and Brill method, and to utilize new instrumentation to calculate liquid holdup, the Mukherjee and Brill (1985) method was developed. Mukherjee and Brill's test facility included an inverted U-shaped, 1.5-in nominal diameter steel pipe that could be raised or lowered at any angle

from 0° to $\pm 90^\circ$ from the horizontal. Approximately 1000 pressure drop measurements and over 1500 liquid holdup measurements were obtained for various gas and liquid flow rates.

The method investigated by Duns and Ros (1963) was as a result of extensive laboratory study in which liquid holdup and pressure gradient were measured. They developed a flow-pattern map that identified flow pattern regions – (I) bubble, plug and part of froth flow regimes, (II) remainder of froth flow and slug flow regimes, (III) mist flow regime - and a transition region. The correlation here is used for pressure loss and holdup with flow regime determination by either the Duns & Ros or the Taitel Dukler correlations. The Duns & Ros method was developed for vertical flow of gas and liquid mixtures in wells.

The Orkiszewski (1967) correlation is used for pressure loss, holdup, and flow regime. The Orkiszewski correlation was developed for the prediction of two phase pressure drops in vertical pipe. Four flow regimes were considered, bubble, slug, annular-slug transition, and annular mist. The method can accurately predict, to within 10%, the two phase pressure drops in naturally flowing and gas lifted production wells over a wide range of well conditions. The precision of the method was verified when its predicted values were compared against 148 measured pressure drops. Unlike most other methods, liquid holdup is derived from observed physical phenomena, and is adjusted for angle of deviation (Schlumberger, 2003).

Most literature on flow geometry and its effect on heat transfer are based on either a mechanistic approach or unified approach. Such can be found in the work of Wang et al (2004).

Chapter 3 Theory

This chapter discusses the mechanics of two-phase gas liquid flows. Basic parameters (such as velocities, flow rates, volume fractions etc) and flow patterns are introduced.

3.1 Two Phase Gas-Liquid Flow

For two-phase flow, mixture expressions for velocities and flow rates must be defined.

3.1.1 Velocities and Flow rates

The superficial velocities of liquid and gas phases (V_{sL} and V_{sG}) are defined as the volumetric flow rate for the phase divided by the pipe cross sectional area (Chen, 2001).

$$V_{sL} = \frac{Q_L}{A} \quad (3.1)$$

$$V_{sG} = \frac{Q_G}{A} \quad (3.2)$$

where Q_L and Q_G are volumetric flow rates of liquid and gas.

The mixture velocity is the sum of the superficial gas and liquid velocities.

$$V_m = V_{sL} + V_{sG} \quad (3.3)$$

Volumetric flow rates for liquid and gas are determined from:

$$Q_L = Q_{Lsc} B_o \quad (3.4)$$

$$Q_G = (Q_{Gsc} - Q_{Lsc} R_s) B_g \quad (3.5)$$

where Q_{Lsc} is oil production rate

Q_{Gsc} is gas production rate.

The no-slip input volume fraction for the liquid and gas phases (λ_L and λ_G) are calculated from:

$$\lambda_L = \frac{Q_L}{Q_L + Q_G} = \frac{V_{sL}}{V_m} \quad (3.6)$$

$$\lambda_G = \frac{Q_G}{Q_L + Q_G} = \frac{V_{sG}}{V_m}$$

During the simultaneous flow of gas and liquid, the lower density and viscosity of the gas phase, which results in higher mobility, enables the gas phase move faster than the liquid phase.

3.1.2 Flow Patterns

Flow patterns describe the geometrical distribution of a multiphase fluid moving through a pipe. This geometric distribution depends on flow rate, fluid properties, and the pipe inclination angle. Various terms are used to explain these flow patterns, and the difference between each one is qualitative and usually relative.

In vertical or moderately deviated pipes (Figure 3-1), the most common flow regimes for gas-liquid mixtures are bubble flow, dispersed bubble flow, plug flow, slug flow, froth flow, mist flow, churn flow and annular flow.

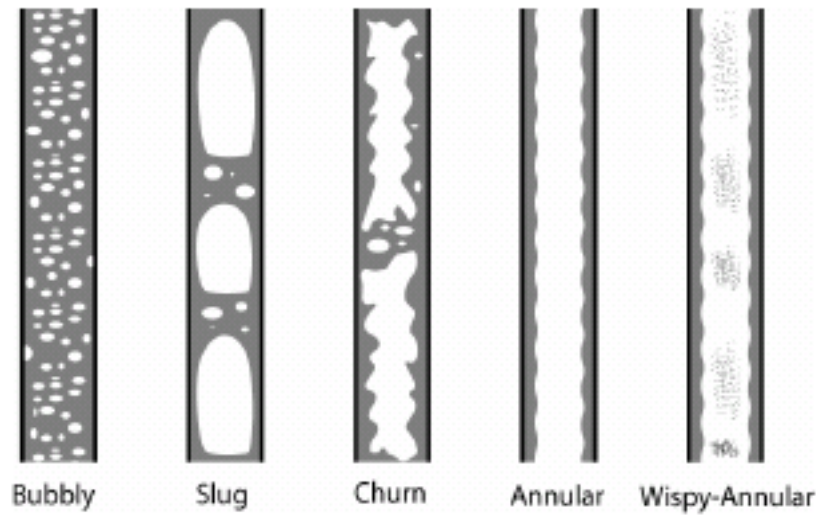


Figure 3-1 Flow Patterns in Vertical and inclined flow (Wang et al, 2004)

In horizontal wells (Figure 3-2), there may be stratified or wavy stratified flow in addition to many of the regimes found in vertical or deviated wells.

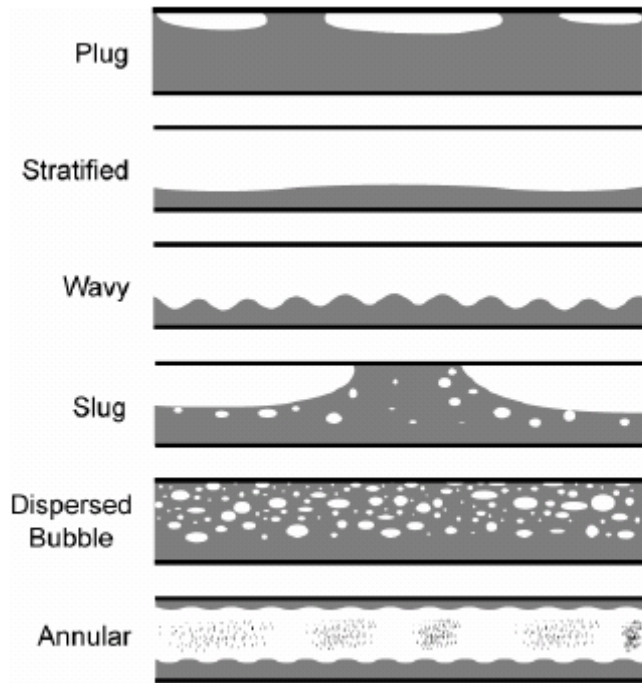


Figure 3-2 Flow Patterns in horizontal and inclined flow (Wang et al, 2004)

One of the important components of a model for 2-phase flow is a method to predict flow patterns. All flow-pattern predictions are based on data from low-pressure systems, with negligible mass transfer between the phases. Hence, these predictions may be inadequate for high temperature, high pressure wells (Brill and Mukherjee, 1999).

Beggs and Brill (1973) suggested three basic flow patterns – segregated, intermittent, and distributed.

In the segregated flow pattern, the gas and liquid phases are continuous, and flow patterns under segregated flow include stratified, wavy, and annular.

Plug and slug flow patterns are found under intermittent flow, and at least one phase (gas or liquid) is discontinuous.

For distributed flow, we have bubble and mist, and the liquid phase is continuous, while the gas phase is discontinuous.

3.1.3 Flow Pattern Maps

Based on the superficial gas and liquid velocities, v_{sG} and v_{sL} , flow pattern maps can be developed. A flow pattern map is a two-dimensional graph that depicts flow regime transition boundaries. The most common parameters used for the axes are v_{sG} and v_{sL} , though dimensionless variables are sometimes utilized. Figure 3-3 shows an experimental flow pattern map in a horizontal setup while Figure 3-4 shows an mechanistic flow pattern map in a slightly downward pipe.

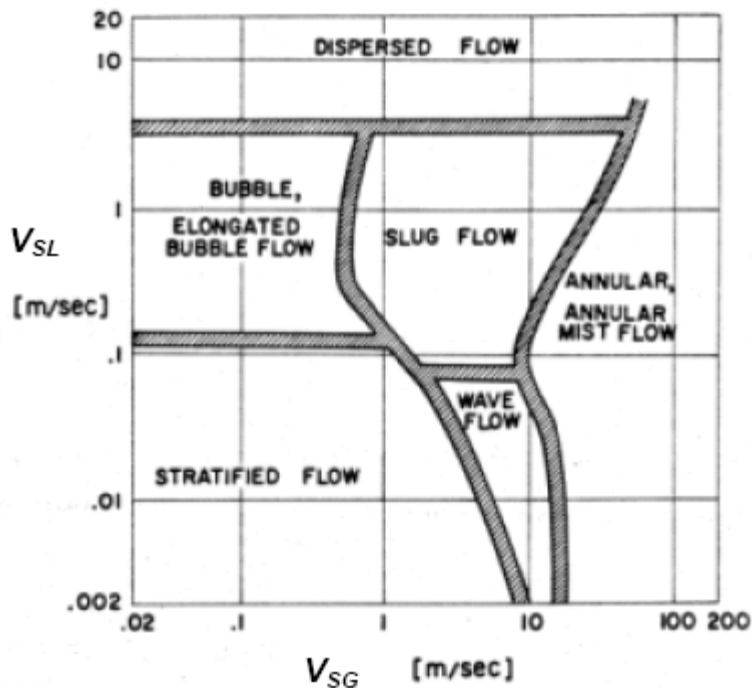


Figure 3-3 Experimental Flow Pattern Map for air-water system in a horizontal pipe (Mandhane, 1974)

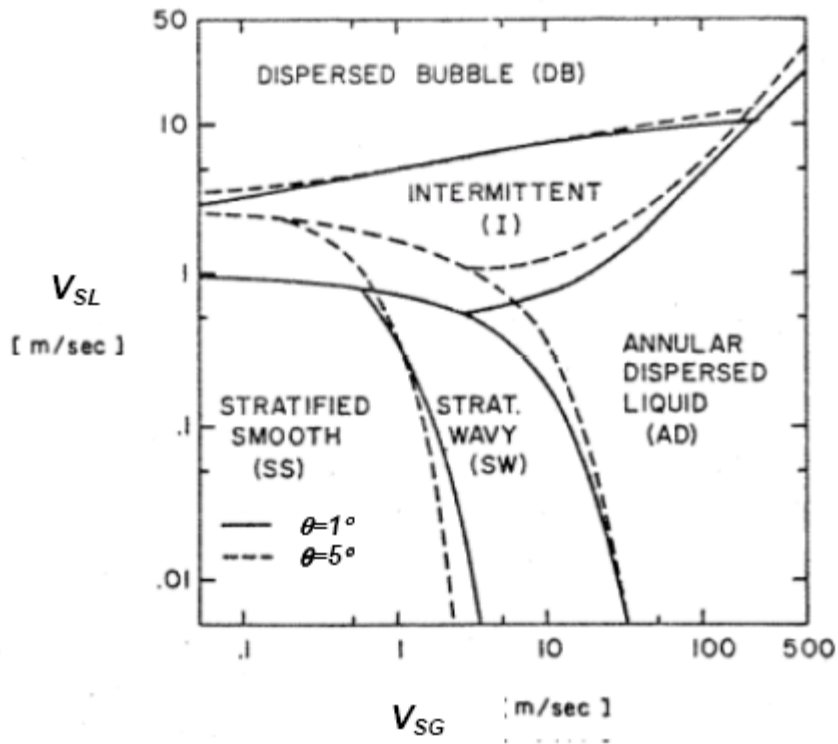


Figure 3-4 Mechanistic Flow Pattern Map for air-water system in a slightly downward pipe (Taitel et al, 1976)

3.1.4 Pressure Gradient

Pressure Gradient is a change in pressure as a function of distance.

$$\left(\frac{dp}{dz}\right)_t = \left(\frac{dp}{dz}\right)_f + \left(\frac{dp}{dz}\right)_{el} + \left(\frac{dp}{dz}\right)_{acc}$$

Where $(dp/dz)_t$ = Total Pressure Gradient (psi/ft)

$(dp/dz)_f$ = Pressure Gradient due to friction (psi/ft)

$(dp/dz)_{el}$ = Pressure Gradient due to elevation (psi/ft)

$(dp/dz)_{acc}$ = Pressure Gradient due to acceleration (psi/ft)

3.1.5 Holdup

In two-phase flow in pipes, the holdup is the fraction of a particular fluid present in an interval of pipe. Each fluid moves at a different speed due to different gravitational forces, with the heavier liquid/oil phase moving slower, or being more held up, than the lighter gas phase. The holdup of a particular fluid is not the same as the proportion of the total flow rate due to that fluid, which is also known as its cut. To determine in-situ flow rates, it is necessary to measure the holdup and velocity of each fluid.

The sum of the holdups of the fluids present is one.

$$H_L + H_G = 1$$

H_L = Liquid holdup

H_G = Gas holdup

3.1.6 Heat Transfer

There are three types of heat transfer modes namely, convection, conduction, and radiation. In pipelines and wellbores, convective heat losses occur between flowing fluids and the pipe wall. In a typical convective heat transfer, a hot surface heats the surrounding fluid, which is then carried away by fluid movement.

Conductive heat losses occur through the pipe wall, any insulation and coating material, and to the environment. Conduction is primarily heat transfer through solids or stationary fluids. Thermal radiation transfer does not require a medium to pass through; thus, it is the only form of heat transfer present in a vacuum. Radiative heat transfer occurs when the emitted radiation (from the sun or environment) strikes the pipeline and is absorbed.

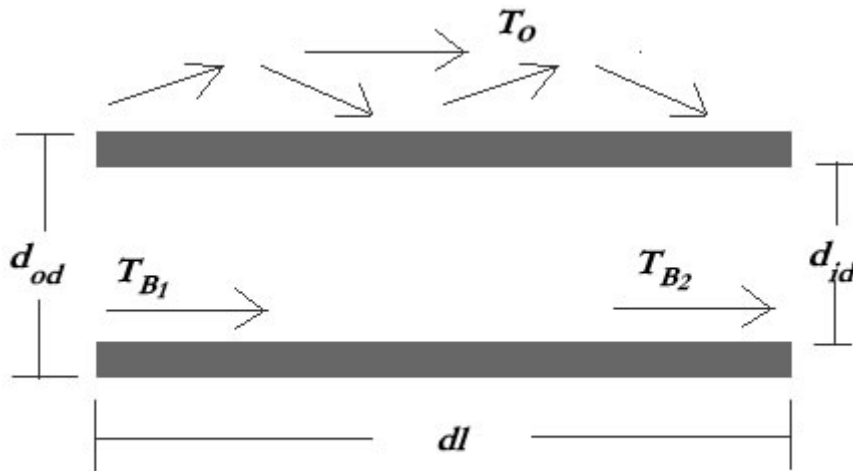


Figure 3-5 Heat transfer setup for a pipe flow.

The heat loss from the fluid in the pipe is equal to the heat absorbed by the environment. Hence, with T_{B1} as inlet temperature, T_{B2} as outlet temperature, v as velocity of the fluid, q as heat flux, ρ as density, dl as length of pipe segment, d_{id} as pipe inner diameter, and c_p as specific heat:

$$(T_{B1} - T_{B2})vA\rho c_p = q\pi d_{id}dl$$

Then,

$$\frac{\delta T_B}{\delta l} = -\frac{q\pi d_{id}}{vA\rho c_p}$$

if $q = U(T_B - T_O)$

Then,

$$\frac{\delta T_B}{\delta l} = -\frac{4U(T_B - T_O)}{d_{id}v\rho c_p}$$

With T_B as bulk temperature of fluid, T_O as surrounding temperature outside pipe, and l is pipe length.

$$U = \frac{1}{\frac{1}{h} + \frac{d_{id}}{2k_p} \ln \frac{d_{od}}{d_{id}} + \frac{d_{id}}{h_o d_{od}}}$$

where U = overall heat transfer

h = internal convective heat transfer

k_p = pipe thermal conductivity

d_{od} = pipe outer diameter

h_o = outside/external convective heat transfer

In this study, the following parameters were assumed:

k_o , oil thermal conductivity = 0.08 Btu/hr/ft/°F

k_g , gas thermal conductivity = 0.02 Btu/hr/ft/°F

c_{pO} , oil heat capacity = 0.08 Btu/lb/°F

c_{pG} , gas heat capacity = 0.02 Btu/lb/°F

Thermal conductivities of the pipes, k_p , can be obtained from Table 3-1 shown below:

Material	Thermal Conductivity Btu/hr/ft/F
Anhydrite	0.75
Carbon Steel	28.9
Concrete Weight Coat	0.81 - 1.15
Corrosion Coat (Bitumen)	0.19
Corrosion Coat (Epoxy)	0.17
Corrosion Coat (Polyurathane)	0.12
Line pipe	27
Mild Steel tubing	26
Neoprene Rubber	0.17
Plastic coated pipe	20
Plastic coated tubing	20
Stainless Steel	8.67
Stainless steel (13%)	18
Stainless steel (15%)	15

Table 3-1 Thermal Conductivities of materials

3.2 Heat Transfer in Two-Phase Flow

As mentioned earlier, many separate studies have been carried out to predict flow patterns and pressure gradients of two-phase gas-liquid flow, and convective heat transfer for pipe flow in two-phase flow. Only few researchers have studied the direct effect of heat transfer correlations on flow geometry. Kim et al (1999) studied 20 heat transfer correlations by comparing experimental data collected from other studies. Suggestions were made for various flow patterns and inclination angles.

A comprehensive mechanistic model was developed by Wang et al (2004) for heat transfer in gas-liquid pipe flow in which the two-phase heat transfer depended on the hydrodynamic behavior of the flow. The prediction of heat transfer correlations used in this study is based on those developed by Wang et al (2004).

Reservoir pressure and temperature, gas specific gravity, oil gravity, gas-oil-ratio, and the water salinity are used to obtain values for gas, oil, and water properties. The equations and correlations used to calculate these values were obtained from technical papers that are well known in the Petroleum, Chemical, and Mechanical Engineering fields. These detailed equations used are shown in appendix B.

3.2.1 Two-Phase Flow Correlations

The aspect of fluid mechanics as it pertains to the project involved the determination of respective fluid velocities, volumetric flow rates, volume fractions, flow pattern, pressure gradient and liquid holdup. The direction of flow (uphill or downhill), the pipe inclination angle, the daily production rate, pipe parameters (such as length, ID, OD, roughness etc), were used to obtain results. The procedures that were used to predict liquid holdup, pressure

gradient, and flow pattern are based on the studies carried out by Beggs and Brill (1973), and Mukherjee and Brill (1985).

3.2.1.1 Beggs and Brill Correlation

In multiphase flow, most of the correlations developed are applicable for vertical and horizontal flow only. The Beggs and Brill (1973) correlation, is one of the few published correlations capable of handling whole range of flow conditions that may be encountered in oil and gas operations, such as uphill, downhill, horizontal, inclined and vertical flow. It was developed using 1" and 1-1/2" sections of pipe that could be inclined at any angle from the horizontal.

The first step is to determine the appropriate flow pattern (Segregated, Intermittent or Distributed) for the particular combination of gas and liquid rates. The liquid holdup, then in-situ density of the gas-liquid mixture is obtained based on the appropriate flow pattern. A two-phase friction factor is calculated based on the gas-liquid ratio and the Fanning friction factor. From this the pressure loss is calculated using gas-liquid mixture properties.

Flow Pattern Map

The Beggs and Brill (1973) correlation requires that a flow pattern be determined. The original flow pattern map has been modified to include a transition zone between the segregated and intermittent flow patterns.

The mixture Froude number, N_{Fr} , and no-slip liquid holdup are used to correlate flow-pattern transition boundaries.

$$N_{Fr} = \frac{v_m^2}{gD}$$

The transition lines for the modified correlation are defined as follows:

$$L_1 = 316\lambda_L^{0.302}$$

$$L_2 = 0.0009252\lambda_L^{-2.4684}$$

$$L_3 = 0.1\lambda_L^{-1.4516}$$

$$L_4 = 0.5\lambda_L^{-6.738}$$

SEGREGATED flow

$$\text{if } \lambda_L < 0.01 \text{ and } N_{Fr} < L_1$$

$$\text{or } \lambda_L \geq 0.01 \text{ and } N_{Fr} < L_2$$

INTERMITTENT flow

$$\text{if } 0.01 \leq \lambda_L < 0.4 \text{ and } L_3 < N_{Fr} \leq L_1$$

$$\text{or } \lambda_L \geq 0.4 \text{ and } L_3 < N_{Fr} \leq L_4$$

DISTRIBUTED flow

$$\text{if } \lambda_L < 0.4 \text{ and } N_{Fr} \geq L_1$$

$$\text{or } \lambda_L \geq 0.4 \text{ and } N_{Fr} > L_4$$

TRANSITION flow

$$\text{if } \lambda_L \geq 0.01 \text{ and } L_2 < N_{Fr} < L_3$$

Liquid Holdup

After the flow geometry has been determined the liquid holdup can be calculated. Beggs and Brill (1973) divided the liquid holdup calculation into two parts. First the liquid holdup for horizontal flow, $HL(0)$, is determined, and then this holdup is modified for inclined flow. $HL(0)$ must be greater than or equal to λ_L , and therefore when $HL(0)$ is smaller than λ_L , $HL(0)$ is assigned a value of λ_L .

$$H_L(0) = \frac{a\lambda_L^b}{N_{Fr}^c}$$

The constants in the above equation are dependent on flow type and given in Table 3-2.

Flow Pattern	a	b	c
Segregated	0.98	0.4846	0.0868
Intermittent	0.845	0.5351	0.0173
Distributed	1.065	0.5824	0.0609

Table 3-2 Beggs and Brill empirical coefficients for H_L

Segregated

$$H_L(0) = \frac{0.98\lambda_L^{0.4846}}{N_{Fr}^{0.0868}}$$

Intermittent

$$H_L(0) = \frac{0.845\lambda_L^{0.5351}}{N_{Fr}^{0.0173}}$$

Distributed

$$H_L(0) = \frac{1.065\lambda_L^{0.5824}}{N_{Fr}^{0.0609}}$$

Transition

$$H_L(0)_{Transition} = AH_L(0)_{Segregated} + BH_L(0)_{Intermittent} \text{ where:}$$

$$A = \frac{L_3 - N_{Fr}}{L_3 - L_2}$$

$$B = 1 - A$$

Once the horizontal in situ liquid volume fraction is determined, the actual liquid volume fraction is obtained by multiplying horizontal holdup ($H_L(0)$) by an inclination factor (Ψ).

$$H_L(\theta) = H_L(0)\Psi$$

where inclination factor is defined as:

$$\Psi = 1 + C \left[\sin(1.8\theta) - \frac{1}{3} \sin^3(1.8\theta) \right]$$

and θ = angle of inclination of pipe

C is a function of flow type, the direction of inclination of the pipe (uphill flow or downhill flow), the liquid velocity number (N_{Lv}), and the mixture Froude Number (N_{Fr}).

$$C = (1 - \lambda_L) \ln(e \lambda_L^f N_{Lv}^g N_{Fr}^h)$$

The values for e, f, g, and h, for the different flow patterns can be obtained from Table 3-3 below.

	Flow Pattern	e	f	g	h
Uphill	Segregated	0.011	-3.378	3.539	-1.614
	Intermittent	2.96	0.305	-0.4473	0.0978
	Distributed	No correction: $\beta = 0, \Psi = 1$			
Downhill	All Patterns	4.7	-0.3692	0.1244	-0.5056

Table 3-3 Beggs and Brill empirical coefficients for C

Where

$$N_{Lv} = 1.938 V_{sL}^4 \sqrt{\frac{\rho_L}{g \sigma_L}}$$

C must always be greater than or equal to zero

Pressure Gradient

The pressure gradient can be calculated after the empirical parameter, S , is obtained.

If $1 < y < 1.2$, then

$$S = \ln(2.2y - 1.2)$$

Otherwise,

$$S = \frac{y}{-0.523 + 3.182 \ln y - 0.8725 (\ln y)^2 + 0.01853 (\ln y)^4}$$

where

$$y = \frac{\lambda_L}{(H_L(\theta))^2}$$

A ratio of the two-phase friction factor to the normalizing friction factor is then defined as follows:

$$\frac{f_{tp}}{f_n} = e^S$$

f_n is obtained through the use of the Fanning friction factor.

The no-slip Reynolds Number is also used, and it is defined as follows:

$$N_{\text{Re}} = \frac{\rho_n v_m d_{id}}{\mu_n}$$

where $\mu_n = \mu_L \lambda_L + \mu_G (1 - \lambda_L)$

The expression for pressure gradient is:

$$\frac{dp}{dL} = \frac{\frac{f \rho_n v_m^2}{2d_{id}} + \rho_s g \sin(\theta)}{1 - E_k}$$

where

$$E_k = \frac{v_m v_{sG} \rho_n}{P_R}$$

3.2.1.2 Mukherjee and Brill Correlation

The Mukherjee and Brill (1985) method attempts to overcome some of the limitations of the Beggs and Brill correlation, and to take advantage of new instrumentation to measure liquid holdup. The Mukherjee and Brill (1985) correlation is capable of handling whole range of flow situations that may be encountered in oil and gas operations, such as uphill, downhill, horizontal, inclined and vertical flow. It was developed using an inverted U-shaped, 1-1/2" nominal ID steel pipe that could be inclined at any angle from 0° to ±90° from horizontal.

Similar to the Beggs and Brill (1973) method, the first step of the Mukherjee and Brill (1985) method is to determine the appropriate flow pattern (Annular Mist, Bubble, Slug or Stratified) for the particular combination of gas and liquid rates. The liquid holdup, then in-situ density of the gas-liquid mixture is then obtained based on the appropriate flow pattern.

A two-phase friction factor is calculated based on the gas-liquid ratio and the Fanning friction factor. From this the pressure loss is calculated using gas-liquid mixture properties.

Flow Pattern Maps

Flow pattern prediction for the Mukherjee and Brill correlation makes use of dimensionless gas and liquid velocity numbers as the x- and y-axes coordinates on a log-log graph.

The following dimensionless parameters were utilized:

$$\text{Liquid Velocity Number, } N_{Lv} = 1.938 v_{sL}^4 \sqrt{\frac{\rho_L}{\sigma_L}}$$

$$\text{Gas Velocity Number, } N_{Gv} = 1.938 v_{sL}^4 \sqrt{\frac{\rho_L}{\sigma_L}}$$

$$\text{Pipe Diameter Number, } N_d = 120.872 d_{id} \sqrt{\frac{\rho_L}{\sigma_L}}$$

$$\text{Liquid Viscosity Number, } N_L = 0.15726 \mu_L^4 \sqrt{\frac{1}{\rho_L \sigma_L^3}}$$

Equations were obtained from the transitional curves. For the bubble/slug transition, we have:

$$N_{Lv/B/S} = 10^x$$

where $x = \log N_{Gv} + 0.940 + 0.074 \sin \theta - 0.855 \sin^2 \theta + 3.695 N_L$

For horizontal and all upflow and downflow angles, the following equation describes the transition for slug/annular mist:

$$N_{GvS/M} = 10^{(1.401-2.694N_L+0.521N_{Lv}^{0.329})}$$

In downflow and horizontal flow, the bubble/slug transition is described by:

$$N_{GvB/S} = 10^y$$

$$y = 0.431 - 3.003N_L - 1.138(\log N_{Lv}) \sin \theta - 0.429(\log N_{Lv})^2 \sin \theta + 1.132 \sin \theta$$

In downflow and horizontal flow, the stratified transition is described by:

$$N_{GvSr} = 10^z$$

$$z = 0.321 - 0.017N_{Gv} - 4.267 \sin \theta - 2.972N_L - 0.033(\log N_{Lv})^2 - 3.925 \sin^2 \theta$$

Liquid Holdup Prediction

The liquid holdup is obtained after the flow pattern is determined. The equation below is used:

$$H_L = e^{\left[(C_1 + C_2 \sin \theta + C_3 \sin^2 \theta + C_4 N_L^2) \left(N_{Gv}^{C_5} / N_{Lv}^{C_6} \right) \right]}$$

Table 3-4 below shows the values for the coefficients used for the holdup calculation.

	Uphill	Downhill Stratified	Downhill Other
C₁	-0.380113	-1.33028	-0.516644
C₂	0.129875	4.808139	0.789805
C₃	-0.119788	4.171584	0.551627
C₄	2.343227	56.26227	15.51921
C₅	0.475686	0.079951	0.371771
C₆	0.288657	0.504887	0.393952

Table 3-4 Mukherjee and Brill Empirical Coefficients for H_L

The flow chart shown below (Figure 3-6) shows the method of prediction of flow patterns by using flow pattern transition equations.

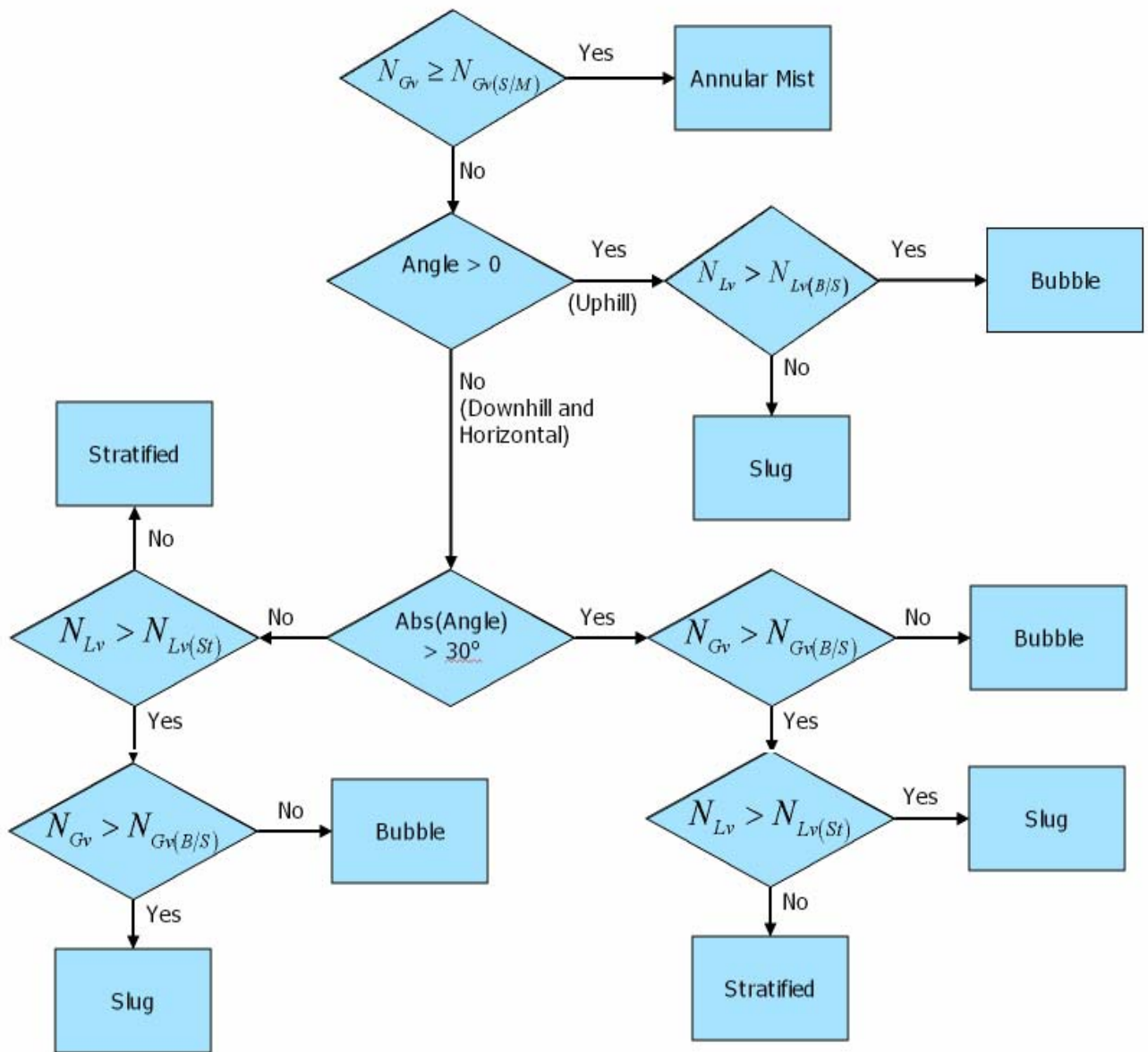


Figure 3-6 Flow chart for the prediction of Mukherjee and Brill Flow Pattern (Brill and Mukherjee, 1999).

Pressure Gradient for the Flow Patterns

Bubble and Slug Flow

$$\frac{dp}{dL} = \frac{\frac{f \rho_s v_m^2}{2d_{id}} + \rho_s g \sin \theta}{1 - E_k}$$

$$\text{where } E_k = \frac{\rho_s v_m v_{sG}}{p}$$

The friction factor, f , is obtained from:

$$\frac{1}{\sqrt{f}} = 1.74 - 2 \log \left(\frac{2\varepsilon}{d_{id}} + \frac{18.7}{N_{Re} \sqrt{f}} \right)$$

Annular Flow

$$\frac{dp}{dL} = \frac{\frac{f \rho_n v_m^2}{2d_{id}} + \rho_s g \sin \theta}{1 - E_k}$$

The friction factor is an empirical expression that depends on liquid holdup. A ratio of holdups, H_R , is obtained, and interpolated from the table below to solve for the friction factor ratio, f_R .

$$H_R = \frac{H_L}{\lambda_L}$$

$$f = f_n(f_R)$$

f_R	H_R
1.00	0.01
0.98	0.20
1.20	0.30
1.25	0.40
1.30	0.50
1.25	0.70
1.00	1.00
1.00	10.00

Table 3-4 Mukherjee and Brill (1999) Annular Flow Friction Factor ratios.

Stratified Flow

According to the Mukherjee and Brill (1985) correlation, stratified flow occurs in highly deviated or horizontal wells. Figure 3-7 shows the control volume that defines all variables for the stratified flow pressure gradient determination.

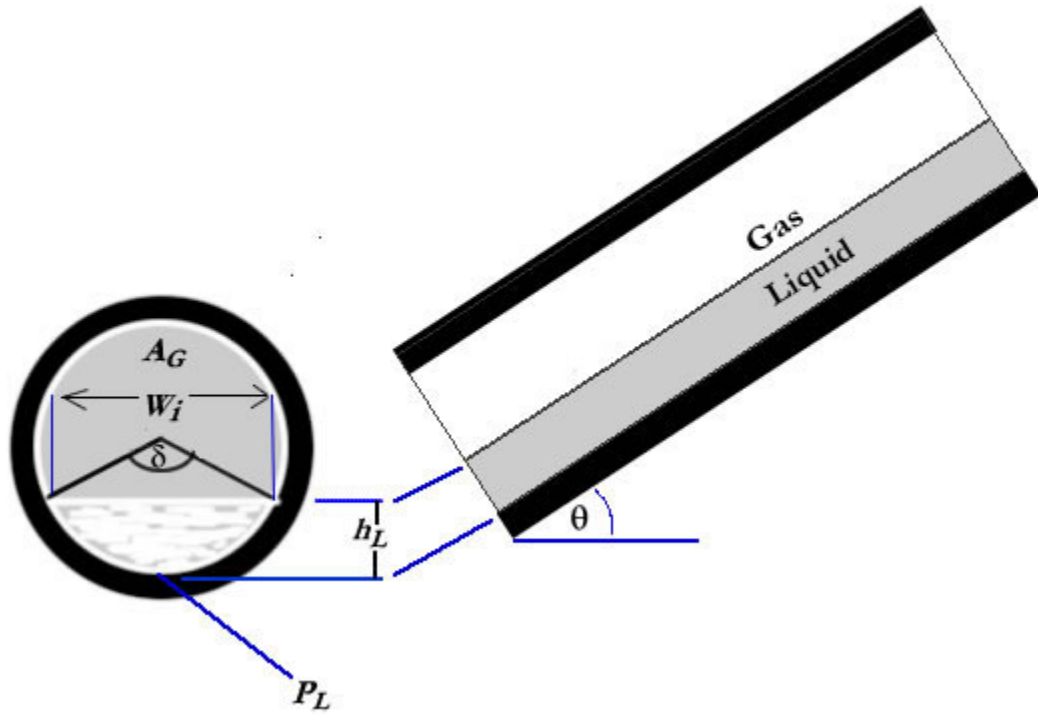


Figure 3-7 Control Volume for Stratified Flow

The equations below are required for pressure gradient calculation.

$$A_G \frac{dp}{dL} = -(\tau_{wG} P_G + \tau_i W_i) - \rho_G A_G g \sin \theta$$

$$A_L \frac{dp}{dL} = -(\tau_{wL} P_L + \tau_i W_i) - \rho_L A_L g \sin \theta$$

An addition of equations $A_G \frac{dp}{dL}$ and $A_L \frac{dp}{dL}$ will yield:

$$A_G \frac{dp}{dL} + A_L \frac{dp}{dL} = -(\tau_{wG} P_G + \tau_i W_i) - \rho_G A_G g \sin \theta + [-(\tau_{wL} P_L + \tau_i W_i) - \rho_L A_L g \sin \theta]$$

Set $\tau_i W_i$ to 0

$$(A_G + A_L) \frac{dp}{dL} = -(\tau_{wG} P_G + 0) - \rho_G A_G g \sin \theta - (\tau_{wL} P_L + 0) - \rho_L A_L g \sin \theta$$

$$A \frac{dp}{dL} = -(\tau_{wG} P_G + \tau_{wL} P_L) - (\rho_G A_G g \sin \theta + \rho_L A_L g \sin \theta)$$

$$A \frac{dp}{dL} = -(\tau_{wL} P_L + \tau_{wG} P_G) - (\rho_L A_L + \rho_G A_G) g \sin \theta$$

$$\delta = 2 \cos^{-1} \left(1 - 2 \frac{h_L}{D} \right)$$

$$H_L = \left(\frac{A_L}{A} \right) = \frac{1}{2\pi} (\delta - \sin \delta)$$

$$P = P_L + P_G$$

$$P_G = \left(1 - \frac{\delta}{2\pi} \right)$$

$$d_{hG} = d_{id} \frac{[2\pi - (\delta - \sin \delta)]}{2\pi - \delta + 2 \sin \frac{\delta}{2}}$$

$$d_{hL} = d_{id} \frac{(\delta - \sin \delta)}{\delta + 2 \sin \frac{\delta}{2}}$$

Mukherjee and Brill (1985) obtained the wall shear stresses from Govier and Aziz (1977).

$$\tau_{wL} = \frac{f_L \rho_L v_L^2}{2g}$$

$$\tau_{wG} = \frac{f_G \rho_G v_G^2}{2g}$$

f_L and f_G are obtained from the friction factor equation, using the Reynolds number based

on:

$$N_{ReL} = \frac{f_L \rho_L d_{hL}}{\mu_L}$$

$$N_{ReG} = \frac{f_G \rho_G d_{hG}}{\mu_G}$$

The liquid and gas velocities, v_L and v_G respectively, are obtained from:

$$v_L = \frac{v_{sL}}{H_L}$$

$$v_G = \frac{v_{sG}}{1 - H_L}$$

The following steps were proposed by Mukherjee and Brill (1999) to obtain the pressure gradient for stratified flow:

1. Use the value H_L to solve iteratively for δ , using 0.001 as an initial value for δ .
2. Use the value for δ obtained from step 1 to obtain h_L/d_{id} . Calculate d_{hG} and d_{hL} .
3. Use δ and P to obtain P_G and P_L .
4. Obtain values for τ_{wL} and τ_{wG} .
5. Calculate pressure gradient from:

$$A \frac{dp}{dL} = -(\tau_{wL} P_L + \tau_{wG} P_G) - (\rho_L A_L + \rho_G A_G) g \sin \theta$$

3.2.2 Pressure Traverse

The pressure traverse procedure for a two-phase gas-liquid flow is a process that calculates the pressure gradient along the pipe length. It uses the pressure gradient equation for a two phase flow (in this case Mukherjee and Brill (1985)), as well as multi-phase flow properties.

The steps listed below are used for the procedure (modified from Vallejo-Arrieta (2002)):

1. Choose pipe length (L), and the length increment (ΔL) for the pipe is computed.
2. Calculate the temperature of the fluids corresponding to the ΔL .

3. Obtain the pressure increment (Δp) corresponding to the length increment (ΔL) using the Mukherjee and Brill (1985) pressure gradient equation and flow properties.
4. Find the average temperature and pressure in the increment.
5. Calculate the fluid properties at the average temperature and pressure from in step 4.
6. Find pressure gradient ($\Delta p/\Delta L$) using fluid properties obtained at average temperature and pressure determined and the Mukherjee and Brill (1985) pressure gradient.
7. Find the pressure increment corresponding to the selected length increment

$$\Delta p = (\Delta p/\Delta L)L$$
8. Compare the estimated Δp and calculated Δp obtained in steps 3 and 7 for tolerance (± 10 psi). If the tolerance does is not appropriate, then use the calculated Δp as the new pressure increment and go to step 4. Iterate steps 4 through 8 until the tolerance is met.
9. Repeat the process from step 2, with $p_{i+1} = p_i + \Delta p_i$ as pressure for the new ΔL .
10. Repeat until the the addition of all the ΔL used is same as the pipe length.

3.2.3 Heat Transfer

This study relied on the research carried out by Wang et al (2004) to predict heat transfer based on flow pattern. Wang et al (2004) developed a unified multiphase heat transfer model for various gas-liquid flow patterns from 0° to $\pm 90^\circ$ from horizontal. The flow patterns modeled are: bubble, annular, stratified, and slug. I assumed annular flow from Wang et al

(2004) to be same as the annular mist flow pattern obtained in the Mukherjee and Brill correlation (1985).

To effectively predict the heat transfer parameters, the flowing temperature of fluids in the pipe has to be determined. The following equation is used:

$$T_2 = T_o + (T_1 - T_o) e^{\left(-\frac{L}{A}\right)}$$

where T_2 = Temperature at Location L, °F

T_1 = Temperature at pipe entrance, °F

T_o = Surrounding temperature, °F

L = distance from pipe entrance, ft

A = Relaxation distance, ft

and, $A = C_1 w^{C_2} \rho_L^{C_3} d_{id}^{C_4} (API)^{C_5} \gamma_g^{C_6}$

where w = total mass flow rate, lbm/sec

$C_1 = 0.0149$

$C_2 = 0.5253$

$C_3 = 2.9303$

$C_4 = 0.2904$

$C_5 = 0.2608$

$C_6 = 4.4146$

Bubble Flow

According to Wang et al (2004), the heat transfer modeling of bubble flow can be assumed to be a pseudo-single-phase flow.

The following equations were utilized:

$$\text{Mixture specific heat: } c_{pm} = (1 - H_L)c_{pG} + H_L c_{pL} \quad (3.1)$$

$$\text{Mixture Reynolds number: } N_{Re_m} = \frac{\rho_m v_m d_{id}}{\mu_L} \quad (3.2)$$

$$\text{Mixture Prandtl number: } N_{Pr} = \frac{c_{pm} \mu_L}{k_L} \quad (3.3)$$

For turbulent flow, the mixture Nusselt number is:

$$N_{Nu_m} = \frac{\left(\frac{f}{2}\right) N_{Re} N_{Pr}}{1.07 + 12.7 \left(\frac{f}{2}\right)^{\frac{1}{2}} (N_{Pr}^{2/3} - 1)} \left(\frac{\mu_L}{\mu_{LW}}\right) \quad (3.4)$$

According to Shah and London (1978), the Nusselt number for bubbly laminar flow is a constant.

$$N_{Nu_m} = 3.657 \quad (3.5)$$

Convective two-phase heat transfer coefficient for bubble flow is:

$$h_m = \frac{N_{Nu_m} k_L}{d_{id}} \quad (3.6)$$

The two-phase overall heat transfer coefficient for bubble flow is:

$$U_m = \frac{1}{\frac{1}{h_m} + \frac{d_{id}}{2k_p} \ln \frac{d_{od}}{d_{id}} + \frac{d_{id}}{h_o d_{od}}} \quad (3.7)$$

Annular/Stratified Flow

In annular/stratified flow, the flow region is divided into two layers, the gas core and the liquid film. The temperatures for the regions are T_c for the gas core and T_f for the liquid film. Figure 3.8 below shows the control volume of temperatures in annular/stratified flow.

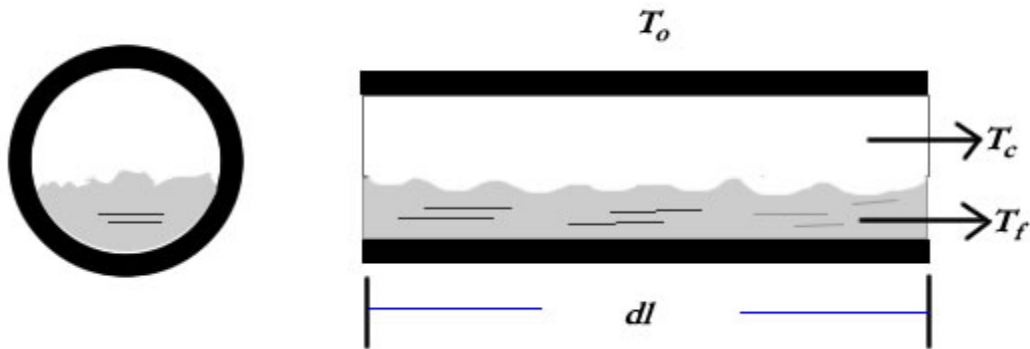


Figure 3-8 Temperature control volume in annular/stratified flow

Reynolds numbers for the gas core and the liquid film are N_{Rec} and N_{Ref} respectively.

The Prandtl numbers are:

$$N_{Pr_c} = \frac{c_{pG} \mu_G}{k_G} \quad (3.9)$$

$$N_{Pr_f} = \frac{c_{pL}\mu_L}{k_L} \quad (3.10)$$

For turbulent flow, the Nusselt numbers are:

$$N_{Nu_f} = \frac{\left(\frac{f}{2}\right) N_{Re_f} N_{Pr_f}}{1.07 + 12.7 \left(\frac{f}{2}\right)^{\frac{1}{2}} (N_{Pr_f}^{2/3} - 1)} \left(\frac{\mu_L}{\mu_{LW}}\right) \quad (3.11)$$

$$N_{Nu_c} = 0.023 N_{Re_c}^{0.8} N_{Pr_c}^{0.3} \quad (3.12)$$

For laminar flow, the Nusselt numbers are:

$$N_{Nu_f} = 3.657 + \frac{7.541 - 3.657}{0.5} (0.5 - \delta) \quad (3.13)$$

$$N_{Nu_c} = 3.657 \quad (3.14)$$

The film and core convective heat transfer coefficients are:

$$h_f = \frac{N_{Nu_f} k_L}{d_{hL}} \quad (3.15)$$

$$h_c = \frac{N_{Nu_c} k_G}{d_{hG}} \quad (3.16)$$

The film and core overall heat transfer coefficients are:

$$U_f = \frac{1}{\frac{1}{h_f} + \frac{d_{id}}{2k_p} \ln \frac{d_{od}}{d_{id}} + \frac{d_{id}}{h_o d_{od}}} \quad (3.17)$$

$$U_c = \frac{1}{\frac{1}{h_c} + \frac{d_{id}}{2k_p} \ln \frac{d_{od}}{d_{id}} + \frac{d_{id}}{h_o d_{od}}} \quad (3.18)$$

The film and core heat fluxes are:

$$q_f = U_f (T_f - T_o) \quad (3.19)$$

$$q_c = U_c (T_c - T_o) \quad (3.20)$$

The two-phase overall heat transfer coefficient for annular/stratified flow is:

$$U_{SA} = \frac{q_f P_L + q_c P_G}{\pi d_{id} \left(\frac{T_f + T_c}{2} - T_o \right)} \quad (3.21)$$

The two-phase convective heat transfer coefficient for annular/stratified flow is:

$$h_{SA} = \frac{1}{\frac{1}{U_{SA}} - \frac{d_{id}}{2k_p} \ln \frac{d_{od}}{d_{id}} - \frac{d_{id}}{h_o d_{od}}} \quad (3.22)$$

The temperature gradient is:

$$\frac{\delta T_{SA}}{\delta l} = - \frac{4U_{SA} (T_{SA} - T_o)}{d_{id} (v_{sL} \rho_L c_{pL} + v_{sG} \rho_G c_{pG})} \quad (3.23)$$

Slug Flow

The two-phase overall heat transfer coefficient for slug flow is:

$$U_s = \frac{A_p \Delta T_s (v_{sL} \rho_L c_{pL} + v_{sG} \rho_G c_{pG})}{\pi d_{id} l (T_s - T_o)} \quad (3.24)$$

The two-phase convective heat transfer coefficient for slug flow is:

$$h_s = \frac{1}{\frac{1}{U_s} - \frac{d_{id}}{2k_p} \ln \frac{d_{od}}{d_{id}} - \frac{d_{id}}{h_o d_{od}}} \quad (3.25)$$

The temperature gradient is:

$$\frac{\delta T_s}{\delta l} = - \frac{4U_s (T_s - T_o)}{d_{id} (v_{sL} \rho_L c_{pL} + v_{sG} \rho_G c_{pG})} \quad (3.26)$$

Chapter 4 Methodology

The aim of this study is to design a computer program called Fluid and Heat Transfer Analyzer (FHTA) that uses empirical formulas or correlations to obtain values for liquid and gas properties, predict two-phase flow pattern and pressure gradient, obtain values for hydrodynamic parameters, carry out a pressure and temperature traverse calculation, predict heat transfer parameters and compare the results based on flow pattern.

Some basic information is required in order to develop such this program. This information bears upon the physical properties of reservoir fluids and rocks, and the ways in which these properties change with the change in pressure and pressure.

The next stage in the development involves the hydrodynamic aspect. This aspect depends on the physical properties of the reservoir fluids and rocks, and also on other properties such as the daily production rate of liquid and gas, the upward or downward flow of the fluids, and the angle of orientation of the pipe.

Results obtained from the second stage are used to predict properties such holdup, pressure gradient, temperature gradient, flow pattern, heat transfer coefficient, etc for different segments of the pipe, along its length. An iterative procedure is used to determine values for some of the parameters. Figure 4.1 shows the flow diagram for the program. Visual Basic programming language was used in the development of the program.

The final stage of the process involved the use of a graph to display the interaction of the properties obtained from the iterative process. The use of 2D, XY-axis system will enable the visualization of plotting one property against another.

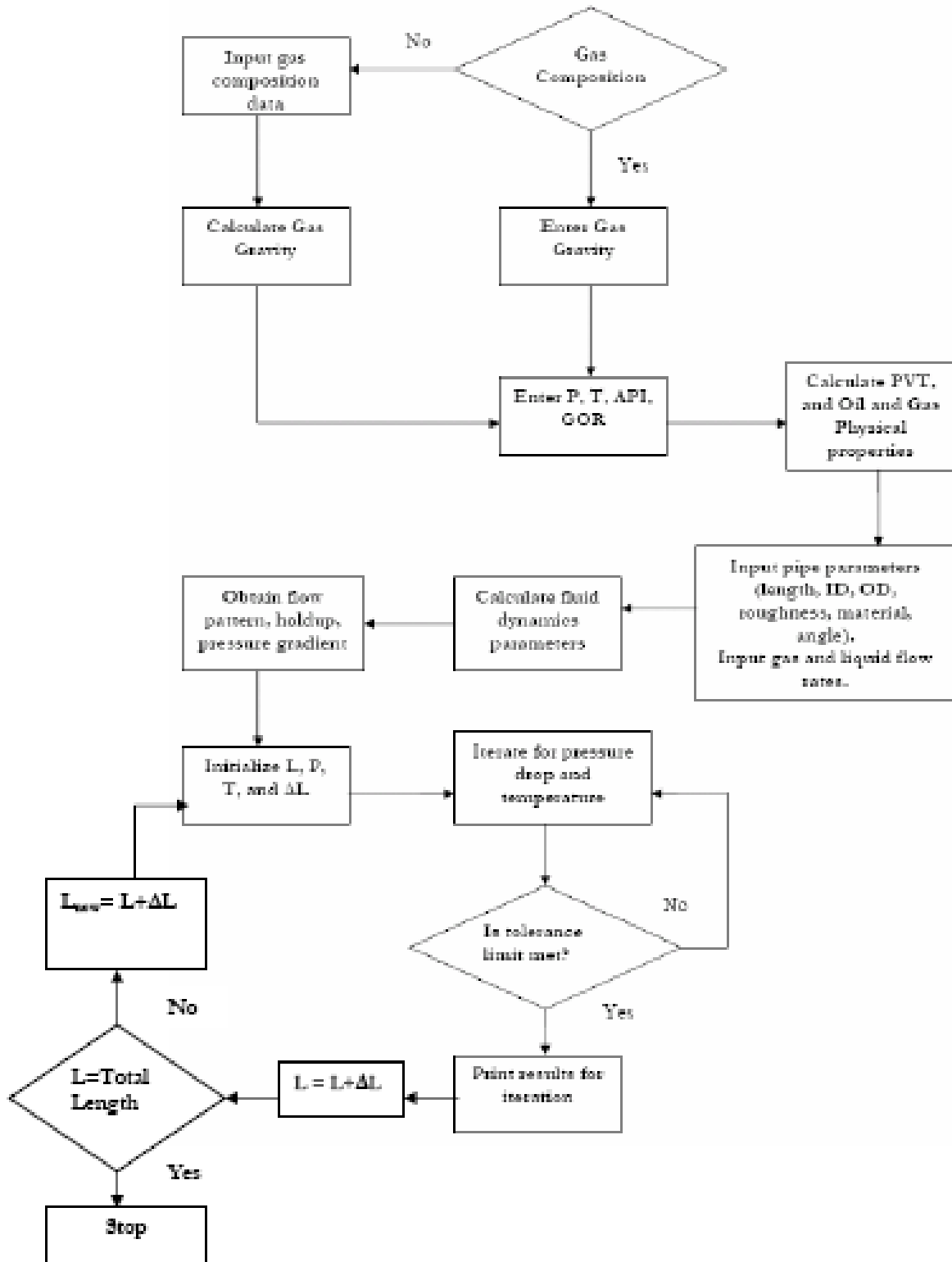


Figure 4-1 Flowchart showing the program setup

4.1 The Graphical User Interface

The software program, Fluid and Heat Transfer Analyzer (FHTA), can be run on any windows based PC, and the results obtained can be exported to a spreadsheet.

An example run is presented using the data given in the table below.

Parameter	Value
Reservoir Pressure, psia	4000
Reservoir Temperature, °F	180
Gas Specific Gravity	0.65
Oil API	30
Initial GOR, SCF/STB	750
Pipe Horizontal Distance	1500
Pipe Length, ft	3000
Pipe ID, in	3.958
Pipe OD, in	4.5
Liquid Surface Tension, dynes/cm	30
Gas Flowrate, SCF/D	5000000
Liquid Flowrate, STB/D	10000
Surface Temperature, °F	100

Table 4-1 Example data for simulation

When the program is initialized, the “Gas Composition Option” window shows up (Figure 4-2). If option yes is chosen for the availability of gas composition information, the “Input Gas Composition Data” window shows (Figure 4-3). Data containing the individual critical temperature and pressure for each constituent of the gas can be imported into the system by clicking on the import button.

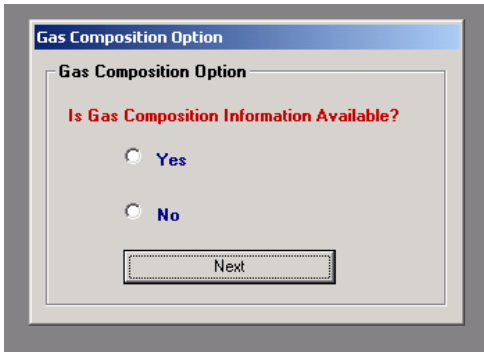


Figure 4-2 Gas composition option

Input Gas Composition Data

Input Gas Composition in Percentage

Gas Type	Percentage %	Individual Gas Gravity	Individual Critical Temperature	Individual Critical Pressure	Pseudocritical Temperature	Pseudocritical Pressure	Gas Gravity
Nitrogen	0.2	0.9672	227.3	493	0.4546	0.986	0.0019344
Carbon Dioxide	4.5	1.5195	547.6	1071	24.642	48.195	0.0683775
Hydrogen Sulphide		1.1765	672.4	1306	0	0	0
Methane	70.5	0.5539	343.04	667.8	241.8432	470.799	0.3904995
Ethane	7	1.0382	549.76	707.8	38.4832	49.546	0.072674
Propane	4.8	1.5225	665.68	616.3	31.95264	29.5824	0.07308
Isobutane	2	2.0068	734.65	529.1	14.693	10.582	0.040136
N-Butane	2	2.0068	765.32	550.7	15.3064	11.014	0.040136
Isopentane	1	2.4911	828.77	490.4	8.287701	4.904	0.024911
N-Pentane	1	2.4911	845.4	486.6	8.454	4.866	0.024911
N-Hexane	2	2.9753	913.4	436.9	18.268	8.738	0.059506
N-Heptane	2.5	3.4596	972.5	396.8	24.3125	9.92	0.08649
N-Octane	1.2	3.9439	1023.89	360.6	12.28668	4.3272	0.0473268
N-Nonane	1.3	4.4282	1070.35	332	13.91455	4.316	.756659E-02
N-Decane		4.9125	1111.8	304	0	0	0
Oxygen		1.1048	278.6	736.9	0	0	0
Hydrogen		0.0696	59.9	188.1	0	0	0
Helium		0.138	9.5	33.2	0	0	0
Water Vapor		0.622	1165.3	3208	0	0	0

Total Mole Fraction, % 100

Total Pseudocritical Temperature 452.8984

Total Pseudocritical Pressure 657.7755

Total Gas Gravity 0.9875487

Wichert-Aziz Correction 7.3563

Corrected Pseudocritical Temperature 445.5421

Corrected Pseudocritical Pressure 647.0915

Buttons: Import Data, Next, Process, Back

Calculated Values

Figure 4-3 Window to input gas composition data

If option “No” is chosen for the availability of gas composition information, the “Input Empirical Gas Gravity” window shows (Figure 4-4), and the gas specific gravity can be inputted.

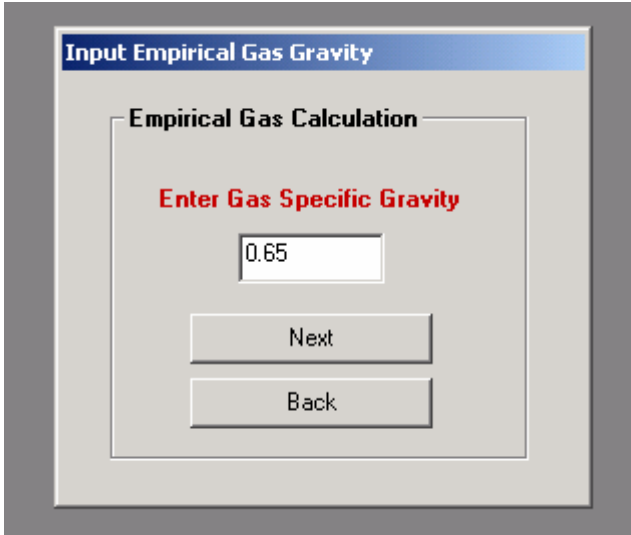


Figure 4-4 Gas specific gravity for empirical correlation

The “Oil and Gas Properties” tab in the “Pressure, Volume, and Temperature” window (Figure 4-5) shows input values for the reservoir temperature, reservoir pressure, oil gravity in API, Gas-Oil ratio, and water salinity. Basic fluid properties are calculated, and the results are shown.

Pressure, Volume, and Temperature

Oil and Gas Properties | Fluid Dynamics

Enter Temperature and Pressure

Reservoir Pressure, psia
 Reservoir Temperature, °F
 Surface Temperature, °F

Gas Properties

Gas Specific Gravity Used

Obtained from your Input Value for Empirical

<input type="text" value="10.733"/>	Gas Density, pound/cu. ft	<input type="text" value="371.2912"/>	Pseudo Critical Temperature
<input type="text" value="0.0217"/>	Gas Viscosity, cp	<input type="text" value="667.7053"/>	Pseudo Critical Pressure
<input type="text" value="0.924"/>	Z Factor	<input type="text" value="1.72"/>	Pseudo Reduced Temperature
<input type="text" value="0.000118"/>	Gas Isothermal Compressibility, 1/psi	<input type="text" value="5.99"/>	Pseudo Reduced Pressure
<input type="text" value="17.039"/>	Gas Molecular Weight	<input type="text" value="0.0014"/>	Gas Formation Volume Factor, cu. ft/SCF

Liquid Properties

Enter Oil Gravity in °API

Enter Initial Gas-Oil Ratio, SCF/STB

Enter Water Salinity, ppm

<input type="text" value="4766.213"/>	Bubble Point Pressure, psia	<input type="text" value="-1.5479"/>	Gas-To-Water Ratio, SCF/STB
<input type="text" value="0.8762"/>	Oil Specific Gravity	<input type="text" value="1.0328"/>	Water Formation Volume Factor, bbl/STB
<input type="text" value="32.7989"/>	Oil Density, pound/cu. ft	<input type="text" value=".3617"/>	Water Viscosity, cp
<input type="text" value="619.1786"/>	Gas-Oil Ratio, SCF/STB	<input type="text" value="60.4167"/>	Water Density, pound/cu. ft
<input type="text" value="1.3906"/>	Oil Formation Volume Factor, bbl/STB	<input type="text" value=".00021"/>	Water Isothermal Compressibility, 1/psi
<input type="text" value=".7214"/>	Oil Viscosity	<input type="text" value="0.3715333"/>	Liquid Viscosity, cp
<input type="text" value=".00004712"/>	Oil Isothermal Compressibility, 1/psi	<input type="text" value="43.2547"/>	Liquid Density, pound/cu. ft
<input type="text" value="1.488"/>	2-Phase Formation Vol., bbl/STB		

Figure 4-5 Oil and Gas Properties window

In the “Fluid Dynamics” tab in the “Pressure, Volume, and Temperature” window (Figure 4.6), values are inputted for the parameters in red. The location of the pipe (air or water), the direction of fluid flow (uphill or downhill), and the pipe material are selected.

The hydrodynamics of the flow are calculated; flow pattern, liquid holdup, and pressure gradient are predicted based on the Beggs and Brill (1973) correlation and the Mukherjee and Brill (1985) correlation.

Pressure, Volume, and Temperature

Oil and Gas Properties

Input Pipe Parameters

3000 Measured Pipe Length, ft 0.00012 Roughness, e, ft

1500 Pipe Distance, ft 30 Liq. Surface Tension, dynes/cm

3.958 Pipe ID, in Pipe in Air
 Pipe in Water

4.5 Pipe OD, in

Select Pipe Material

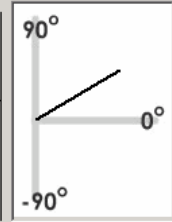
Anhydrite

Fluid Dynamics

Computes Angle of Inclination

θ .Degrees
29.99995

Is the Flow Uphill or Downhill?
 Uphill
 Downhill



If angle is positive, then uphill option
If angle is negative, then downhill option

Input Gas and Liquid Flow Rates

5000000 Gas Flow Rate, SCF/D 10000 Oil Flow Rate, STB/D

Gas and Liquid Phase Results

6.32E-02 Volumetric Gas Flow Rate, cu. ft/sec 9.04E-01 Volumetric Oil Flow Rate, cu. ft/sec

7.40E-01 Superficial Gas Velocity, ft/sec 1.06E+01 Superficial Oil Velocity, ft/sec

6.54E-02 Input Vol. Fraction (gas) 9.35E-01 Input Vol. Fraction (oil)

Mixture Results

11.3156 Mixture Velocity, ft/sec

Beggs-Brill Results

Distributed Flow Pattern

.87977 Liquid Holdup

.18863 Pressure Gradient, psi/ft

Mukherjee-Brill Results

Bubble Flow Pattern

.84004 Liquid Holdup

.17675 Pressure Gradient, psi/ft

Calculate Iteration

Figure 4-6 Fluid Dynamics window

The “Iteration Results” tab in “Results” window (Figure 4-7) shows a table that consists of results for the pressure and temperature iterative procedure as functions of length increments, hydrodynamics - v_{sG} , v_{sL} , and holdup, pressure gradient, and fluid pattern (based on the Mukherjee and Brill correlation (1985)), and thermal properties – temperature gradient, two-phase convective heat transfer coefficient, and the overall heat transfer coefficient.

Iteration Results

Graph and Export to Spreadsheet

Length	Pressure	Temperature	HL	IREG	VSL	VSG	ELGR	FRGR	ACCGR	Total GR
150.000	3972.227	178.000	1.0000	Bubble	9.5478	0.00E+00	0.1634	0.0217	0.00E+00	0.1850
300.000	3944.396	174.000	1.0000	Bubble	9.5293	0.00E+00	0.1637	0.0218	0.00E+00	0.1850
450.000	3916.504	170.000	1.0000	Bubble	9.5110	0.00E+00	0.1641	0.0219	0.00E+00	0.1850
600.000	3888.550	166.000	1.0000	Bubble	9.4926	0.00E+00	0.1644	0.0220	0.00E+00	0.1850
750.000	3860.535	162.000	1.0000	Bubble	9.4743	0.00E+00	0.1647	0.0221	0.00E+00	0.1850
900.000	3832.457	158.000	1.0000	Bubble	9.4561	0.00E+00	0.1650	0.0222	0.00E+00	0.1850
1050.000	3804.315	154.000	1.0000	Bubble	9.4379	0.00E+00	0.1653	0.0223	0.00E+00	0.1850
1200.000	3776.107	150.000	1.0000	Bubble	9.4198	0.00E+00	0.1657	0.0224	0.00E+00	0.1850
1350.000	3747.832	146.000	1.0000	Bubble	9.4017	0.00E+00	0.1660	0.0225	0.00E+00	0.1850
1500.000	3719.487	142.000	1.0000	Bubble	9.3836	0.00E+00	0.1663	0.0227	0.00E+00	0.1850
1650.000	3691.071	138.000	1.0000	Bubble	9.3656	0.00E+00	0.1666	0.0228	0.00E+00	0.1850
1800.000	3662.583	134.000	1.0000	Bubble	9.3476	0.00E+00	0.1669	0.0230	0.00E+00	0.1850
1950.000	3634.019	130.000	1.0000	Bubble	9.3297	0.00E+00	0.1673	0.0232	0.00E+00	0.1900
2100.000	3605.378	126.000	1.0000	Bubble	9.3118	0.00E+00	0.1676	0.0234	0.00E+00	0.1900
2250.000	3576.656	122.000	1.0000	Bubble	9.2940	0.00E+00	0.1679	0.0236	0.00E+00	0.1910
2400.000	3547.850	118.000	1.0000	Bubble	9.2761	0.00E+00	0.1682	0.0238	0.00E+00	0.1920
2550.000	3518.957	114.000	1.0000	Bubble	9.2584	0.00E+00	0.1685	0.0241	0.00E+00	0.1920
2700.000	3489.973	110.000	1.0000	Bubble	9.2406	0.00E+00	0.1689	0.0244	0.00E+00	0.1930
2850.000	3460.892	106.000	1.0000	Bubble	9.2230	0.00E+00	0.1692	0.0247	0.00E+00	0.1930
3000.000	3431.710	102.000	1.0000	Bubble	9.2053	0.00E+00	0.1695	0.0250	0.00E+00	0.1940

Process

Figure 4-7 Window showing pressure and temperature iteration, hydrodynamics, and thermal properties based on pipe length

Graphs can be plotted to visualize the relationship between the parameters. Figure 4-8 shows a plot of length (ft) against temperature gradient ($^{\circ}\text{F}/\text{ft}$) for a 3000 ft long pipeline.

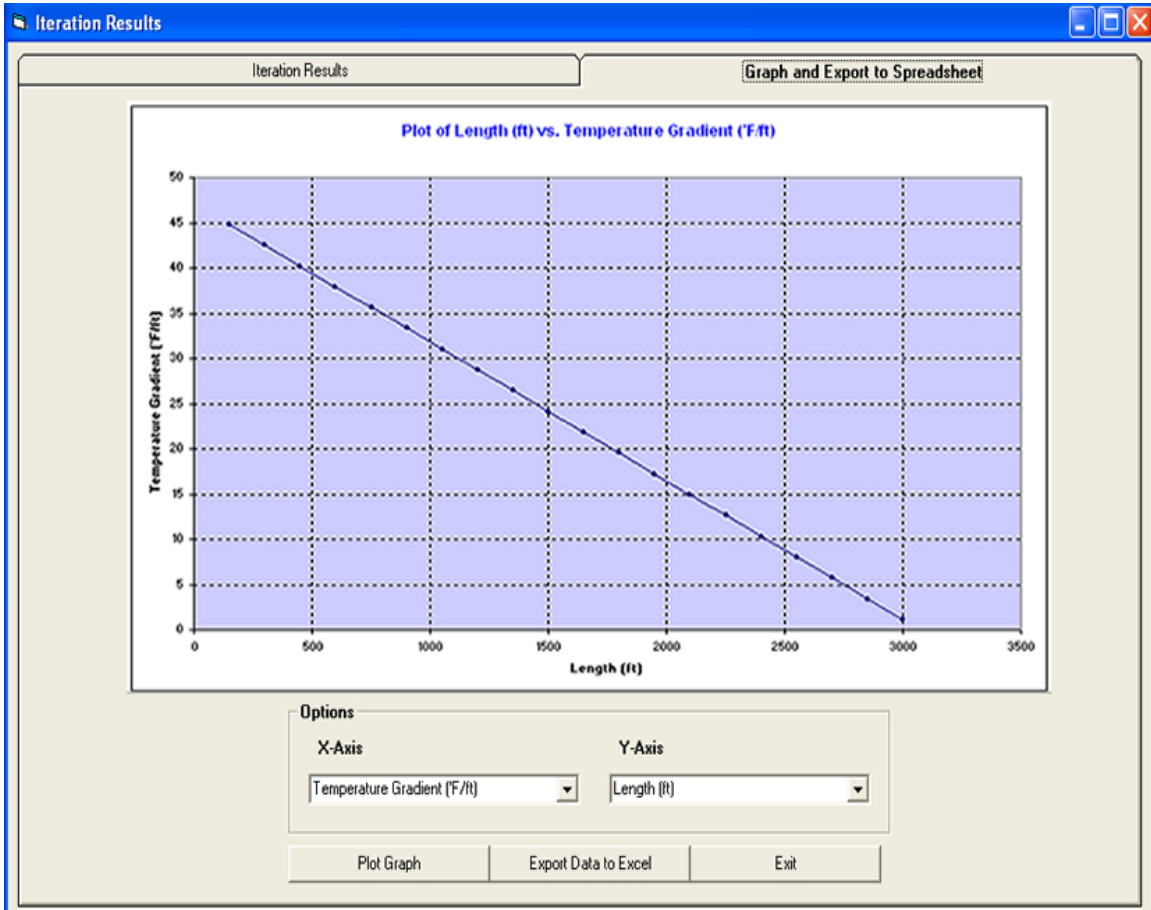


Figure 4-8 Variation of temperature gradient ($^{\circ}\text{F}/\text{ft}$) with pipe length (ft)

The data from the "Iteration Results" tab in "Iteration Results" window, PVT calculations and hydrodynamic predictions can be exported into Microsoft Excel spreadsheet. The iteration data is loaded onto a sheet called "Iteration Results" (Figure 4-9), and the PVT and fluid dynamics is loaded to a sheet called "Key Values" (Figure 4-10).

Microsoft Excel - Exported Results.xls

File Edit View Insert Format Tools Data Window Help

Paste All Items

100%

Surf Csg tbg Perf CIBP Pkr TAC Arial 10 B I U \$ % , ' " . : ;

	A	B	C	D	E	F	G	H	I	J	K	L	M	N
1	Length	Pressure	Temperature	HL	IREG	VSL	VSG	ELGR	FRGR	ACCGR	Total GR	TEMPGR	U	H
2	150	3972.227	178	1	Bubble	9.5478	0.00E+00	0.1634	0.0217	0.00E+00	0.1852	44.7964	0.7981	0.887
3	300	3944.396	174	1	Bubble	9.5293	0.00E+00	0.1637	0.0218	0.00E+00	0.1855	42.4992	0.7981	0.887
4	450	3916.504	170	1	Bubble	9.511	0.00E+00	0.1641	0.0219	0.00E+00	0.1859	40.2019	0.7981	0.887
5	600	3888.55	166	1	Bubble	9.4926	0.00E+00	0.1644	0.022	0.00E+00	0.1864	37.9047	0.7981	0.887
6	750	3860.535	162	1	Bubble	9.4743	0.00E+00	0.1647	0.0221	0.00E+00	0.1868	35.6074	0.7981	0.887
7	900	3832.457	158	1	Bubble	9.4561	0.00E+00	0.165	0.0222	0.00E+00	0.1872	33.3102	0.7981	0.887
8	1050	3804.315	154	1	Bubble	9.4379	0.00E+00	0.1653	0.0223	0.00E+00	0.1876	31.0129	0.7981	0.887
9	1200	3776.107	150	1	Bubble	9.4198	0.00E+00	0.1657	0.0224	0.00E+00	0.1881	28.7157	0.7981	0.887
10	1350	3747.832	146	1	Bubble	9.4017	0.00E+00	0.166	0.0225	0.00E+00	0.1885	26.4184	0.7981	0.887
11	1500	3719.487	142	1	Bubble	9.3836	0.00E+00	0.1663	0.0227	0.00E+00	0.189	24.1212	0.7981	0.887
12	1650	3691.071	138	1	Bubble	9.3656	0.00E+00	0.1666	0.0228	0.00E+00	0.1894	21.8239	0.7981	0.887
13	1800	3662.583	134	1	Bubble	9.3476	0.00E+00	0.1669	0.023	0.00E+00	0.1899	19.5267	0.7981	0.887
14	1950	3634.019	130	1	Bubble	9.3297	0.00E+00	0.1673	0.0232	0.00E+00	0.1904	17.2294	0.7981	0.887
15	2100	3605.378	126	1	Bubble	9.3118	0.00E+00	0.1676	0.0234	0.00E+00	0.1909	14.9322	0.7981	0.887
16	2250	3576.656	122	1	Bubble	9.294	0.00E+00	0.1679	0.0236	0.00E+00	0.1915	12.6349	0.7981	0.887
17	2400	3547.85	118	1	Bubble	9.2761	0.00E+00	0.1682	0.0238	0.00E+00	0.192	10.3376	0.7981	0.887
18	2550	3518.957	114	1	Bubble	9.2584	0.00E+00	0.1685	0.0241	0.00E+00	0.1926	8.0404	0.7981	0.887
19	2700	3489.973	110	1	Bubble	9.2406	0.00E+00	0.1689	0.0244	0.00E+00	0.1932	5.7431	0.7981	0.887
20	2850	3460.892	106	1	Bubble	9.223	0.00E+00	0.1692	0.0247	0.00E+00	0.1939	3.4459	0.7981	0.887
21	3000	3431.71	102	1	Bubble	9.2053	0.00E+00	0.1695	0.025	0.00E+00	0.1946	1.1486	0.7981	0.887
22														

Figure 4-9 Iteration results

Microsoft Excel - Exported Results.xls

File Edit View Insert Format Tools Data Window Help

Paste All Items

100%

Surf Csg tbg Perf CIBP Pkr TAC Arial 10 B I U

	A	B	C	D	E	F	G	H
1	Key Values							
2								
3	Reservoir Pressure, psia	4000	Liquid Surface Tension, dynes/cm		30			
4	Reservoir Temperature, F	180	Gas Flowrate, SCF/D		5000000			
5	Gas Specific Gravity	0.65	Liquid Flowrate, STB/D		10000			
6	Oil API	30	Vol Gas Flowrate, cu. ft/sec		6.32E-02			
7	Initial GOR, SCF/STB	750	Vol Liquid Flowrate, cu. ft/sec		9.04E-01			
8	Z factor	0.924	Superficial Gas Velocity, ft/sec		7.40E-01			
9	Gas Density, lb/cu. ft	10.733	Superficial Liquid Velocity, ft/sec		1.06E+01			
10	Gas Viscosity, cp	0.0217	Mixture Velocity, ft/sec		11.3156			
11	Liquid Density, lb/cu. ft	43.2547	Whole pipe Beggs & Brill Liquid Holdup		0.87977			
12	Liquid Viscosity, cp	0.3715333	Whole pipe Beggs & Brill Pressure Gradient		0.18863			
13	Pipe Inclination Angle	29.99995	Whole pipe Mukherjee & Brill Liquid Holdup		0.84004			
14	Pipe Length, ft	3000	Whole pipe Mukherjee & Brill Pressure Gradient		0.17675			
15	Pipe ID, in	3.958	Pipe Inlet Pressure, psia		4000			
16	Pipe OD, in	4.5	Pipe Inlet Temperature, F		180			
17								
18								
19								
20								
21								
22								
23								
24								

Figure 4-10 Key values

4.2 Relationships between results obtained

The results obtained from the software designed in this study were extracted and set up against variables and constants with the aim of understanding how they affect one another.

Data used is given in Table 4.1.

4.2.1 Angles, holdup and pressure gradient

The liquid holdup and pressure gradient were plotted against a range of angles for the example run with data given in Table 4-1. It was found that the direction of flow (upflow or downflow) affects the flow pattern. For upflow, the flow pattern obtained was slug, and bubble flow was observed in downflow. It was also observed that pressure gradient (Figure 4-11) increased as the angle of inclination moved from negative values to positive values, while liquid holdup remained almost constant (Figure 4-12).

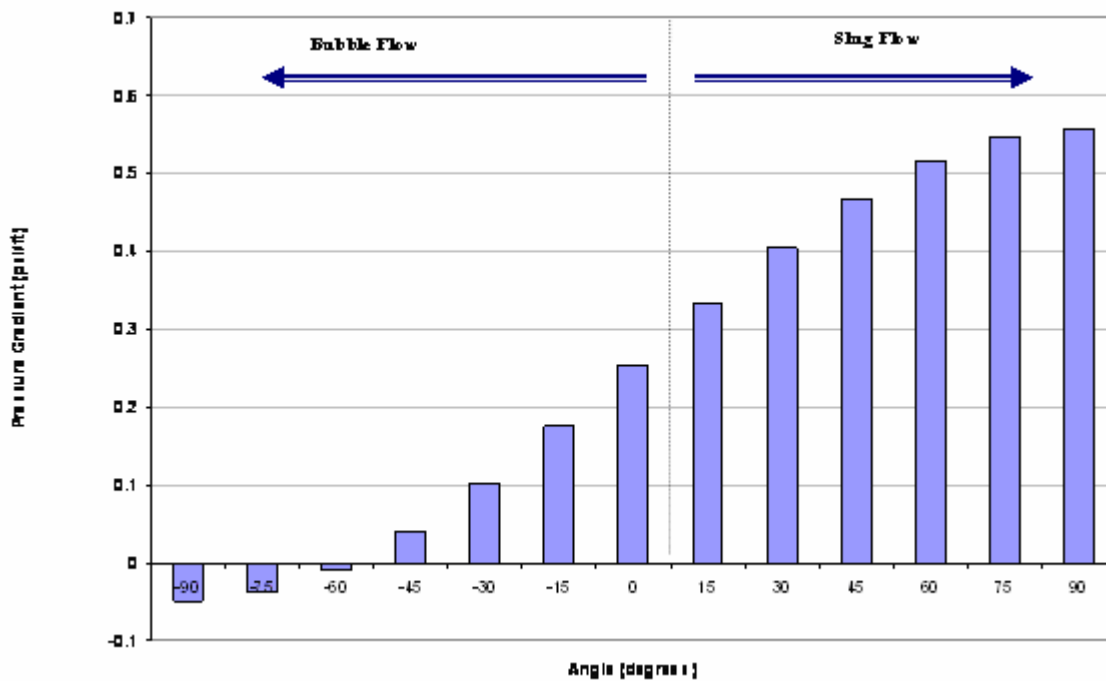


Figure 4-11 Variation of pressure gradient with pipe inclination angle

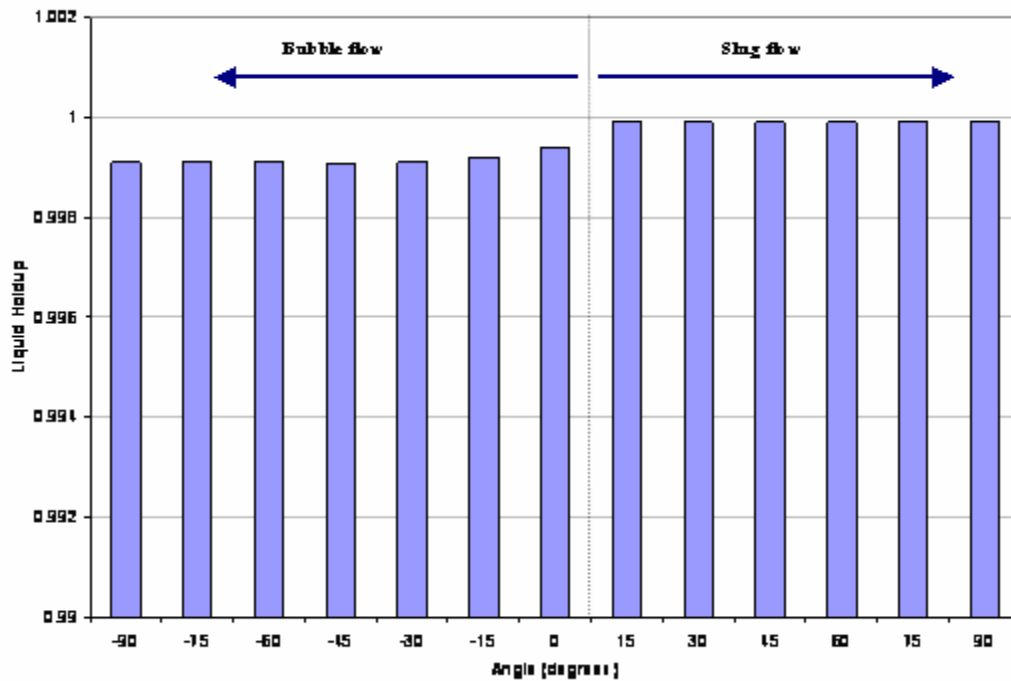


Figure 4-12 Variation of holdup with pipe angle

The program designed in this project shows that values for holdup and pressure gradient obtained from the Beggs and Brill (1973) correlation were slightly lower than those obtained from the Mukherjee and Brill (1985) method. The pressure gradient in both cases increased with an increase in angle, while the holdup remained almost constant. This relationship can be seen in Figures 4-13 and 4-14.

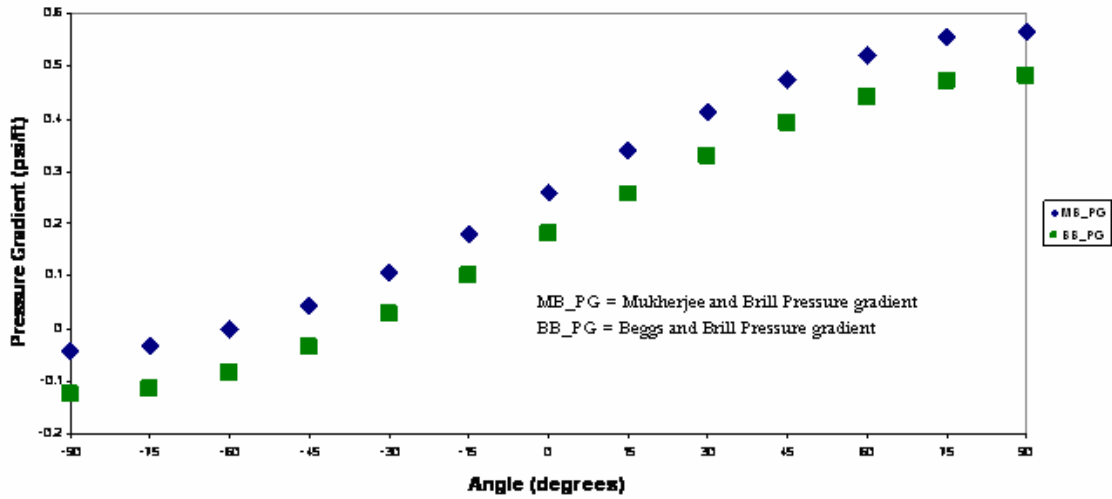


Figure 4-13 Mukherjee & Brill and Beggs & Brill (Pressure Gradient) against pipe angle

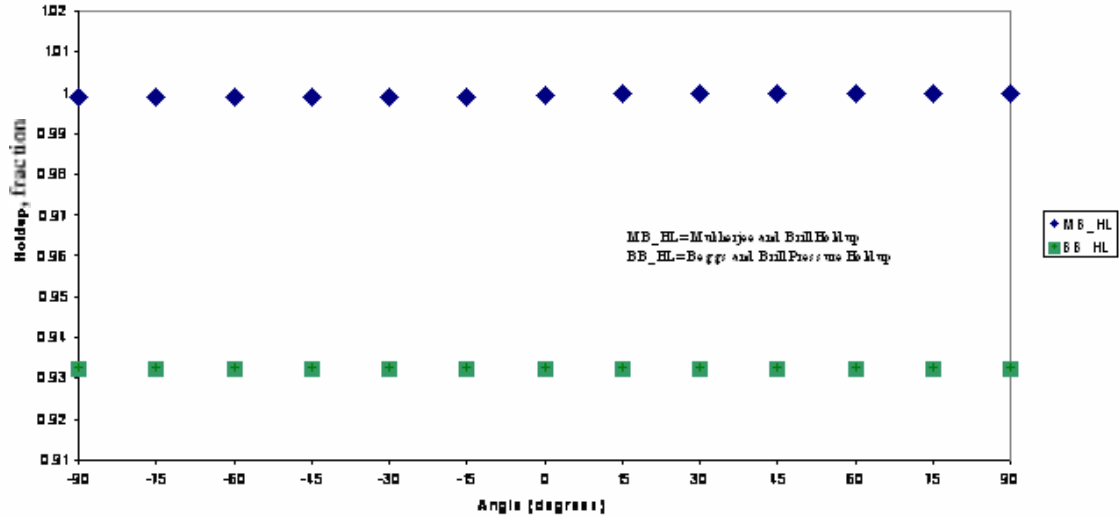


Figure 4-14 Beggs & Brill and Mukherjee & Brill (Holdup) against pipe angle

Stratified flow was found to occur in large diameter pipes, at increased gas production rates, and in highly deviated inclinations. For a pipe ID of 3.958 in, gas flow rate of 7.5 MMscf/Day, liquid production rate of 10000 STB/Day, stratified flow occurred at an angle range of $-30^\circ \leq \theta \leq -21^\circ$. As the pipe diameter and gas production rate are increased, the range of inclination increases, and the maximum range obtained is $-75^\circ \leq \theta \leq -10^\circ$.

4.2.2 Heat Transfer and Flow Pattern

Bubble flow is treated as a pseudo-single phase flow; hence the heat transfer parameters remain constant along the length of the pipe. This can be observed in Fig. 4-15 below.

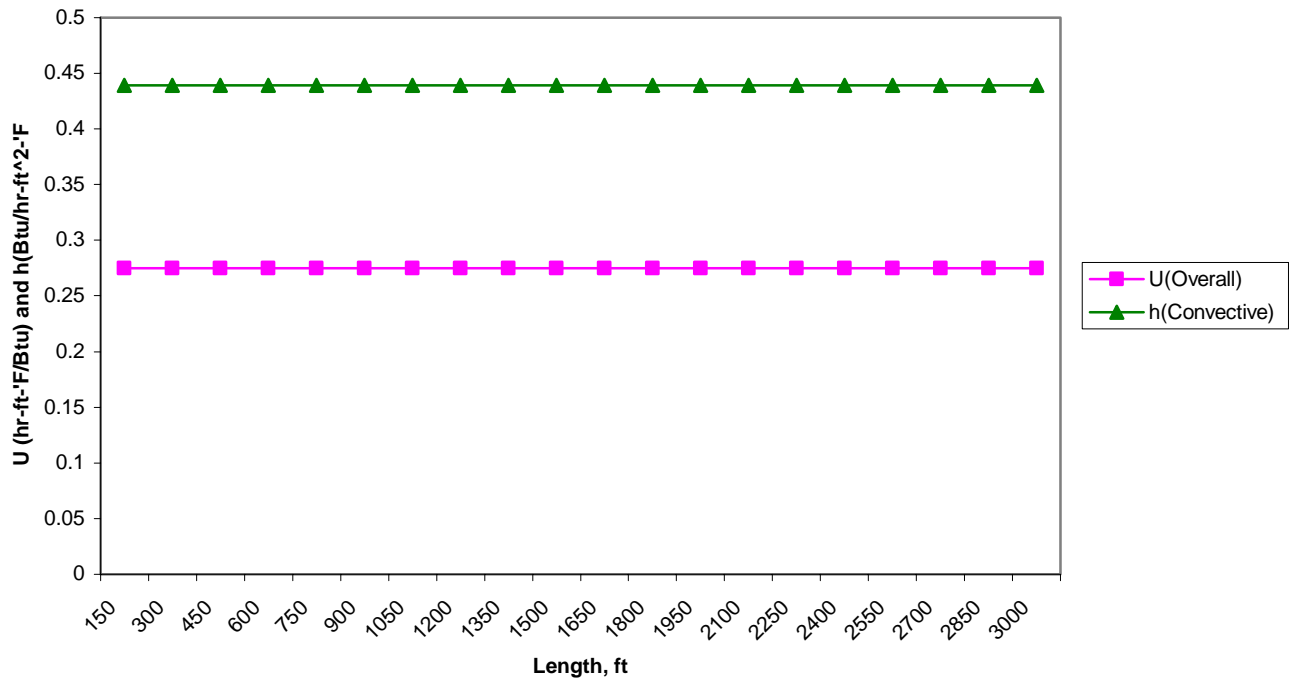


Figure 4-15 Relationship between overall coefficient of heat transfer (U) and convective coefficient of heat transfer (h) for bubble flow

In slug flow, the slug region and the film region were considered as being homogenous for this study. The heat transfer parameters for the entire slug unit are based on the temperature of the entire pipe length, and the surrounding temperature outside the pipe. The temperature parameters obtained is an approximate average for the pipe segments.

For a stratified flow, the heat transfer parameters are also based on the entire pipe length, and the constant values obtained for overall coefficient of heat transfer (U) and the convective coefficient of heat transfer (h) are approximate average values for the entire pipe segments. The same relationship will exist for annular/mist because the same procedure whereby the heat transfer of the gas and liquid phases were analyzed separately, and unified to obtain general equations.

4.2.3 Comparison with PipeSim

In order to test the validity of the results from the developed program, runs were conducted with a commercially available software. Schlumberger owns and designs a commercial software known as PipeSim. This program is a production systems analysis software that provides steady-state, multiphase flow simulation for oil and gas production systems.

The simulations and results obtained in the software designed in this study were compared to those in PipeSim. The comparison shows a high level of agreement.

Table 4-2 below shows the input values used.

Parameter	Value
Pipe Inlet Pressure, psia	1700
Pipe Inlet Temperature, °F	180
Gas Specific Gravity	0.7
Oil °API	33
Initial GOR, SCF/STB	1000
Pipe Inclination Angle, degrees	1
Pipe Length, ft	15000
Pipe ID, in	6
Pipe OD, in	6.5
Liquid Surface Tension, dynes/cm	8.41
Gas Flowrate, SCF/D	1.00E+07
Liquid Flowrate, STB/D	10000

Table 4-2 Input values for comparison with PipeSim

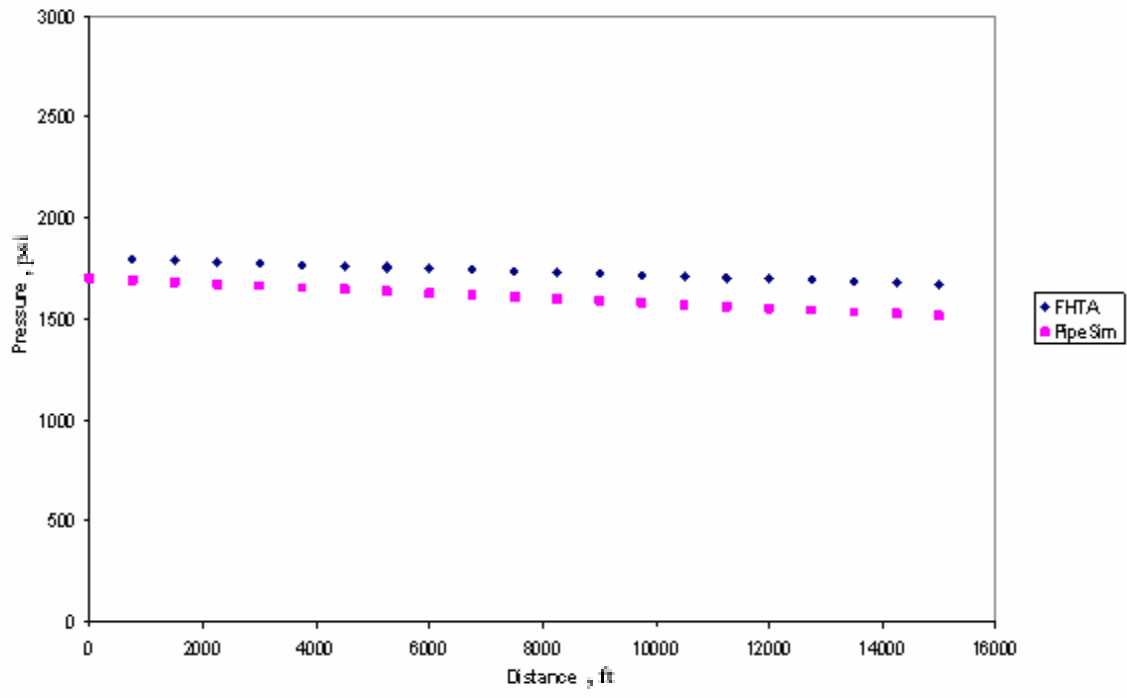


Figure 4-16 Variation of pressure along pipe length for PipeSim and FHTA

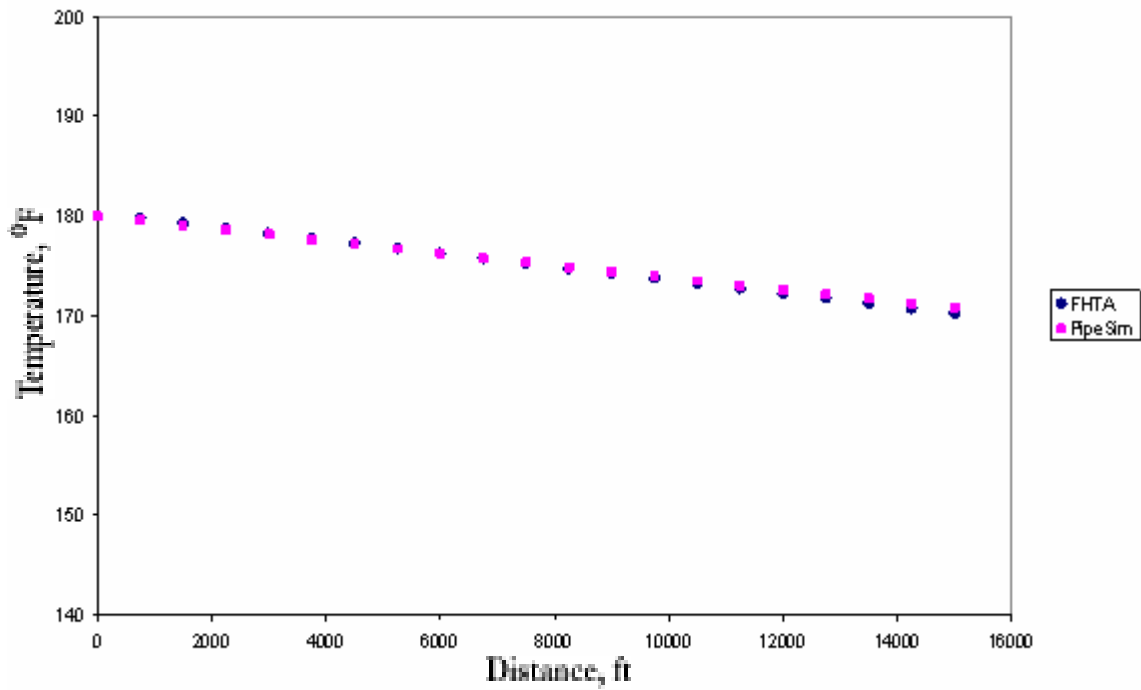


Figure 4-17 Variation of temperature along pipe length for PipeSim and FHTA

4.3 Sensitivity Runs

Effect of Temperature

The effect of inlet temperature on pressure (p), temperature gradient (dT/dL), and liquid holdup (H_L) was investigated. The ambient temperature was kept constant at 90°F, while the inlet temperature was varied from 100°F to 300°F, with increments of 50°F. The pipe is set at both horizontal (pipeline) position (0°) and at vertical (wellbore) position (90°). The data used is shown below in Table 4-3.

Parameter	Value
Reservoir Pressure, psia	4000
Gas Specific Gravity	0.65
Oil API	30
Initial GOR, SCF/STB	750
Pipe Inclination Angle, degree	0, 90
Pipe Length, ft	10000
Pipe ID, in	3.958
Pipe OD, in	4.5
Liquid Surface Tension, dynes/cm	30
Gas Flowrate, SCF/D	5000000
Liquid Flowrate, STB/D	10000

Table 4-3 Input values for sensitivity runs.

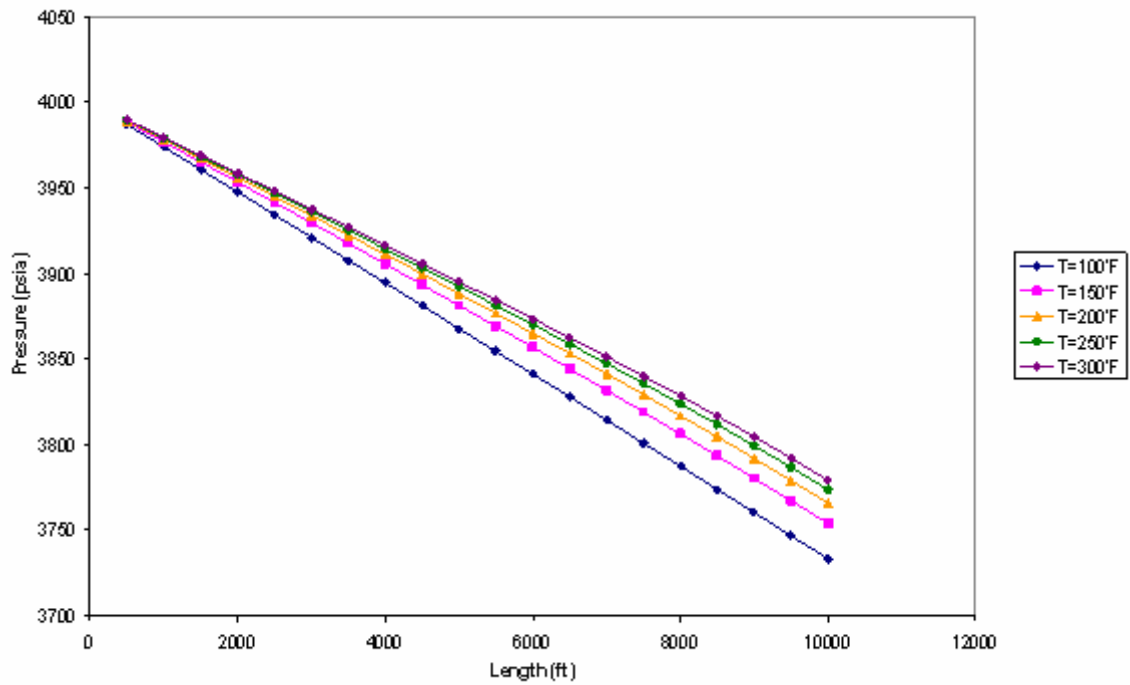


Figure 4-18 Variation of pressure with pipe length for various reservoir temperatures

As observed in Figure 4-18, lower inlet temperatures yield lower pressure values than higher temperatures along the length of the pipe. As the inlet temperature increases, the results for the final pressure values begin to converge.

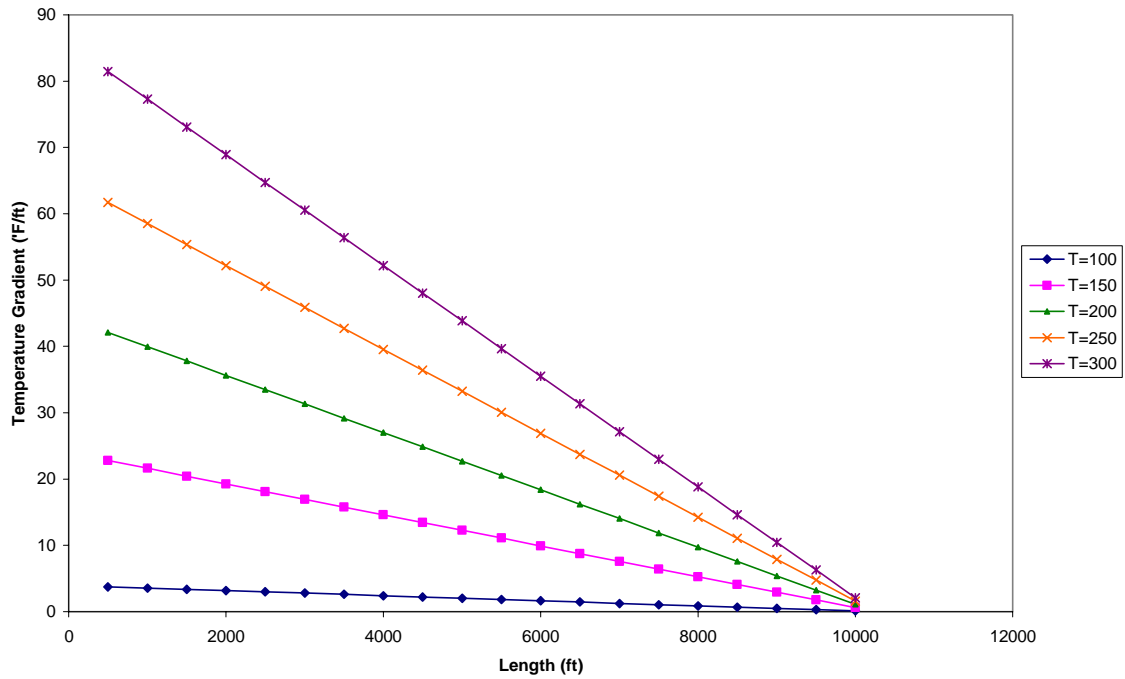


Figure 4-19 Variation of temperature gradient with pipe length for various reservoir temperatures

Temperature gradient decreases gradually along the length of the pipe. At lower reservoir temperatures, the change in temperature is slight. As temperature increases, the values for temperature gradient increase.

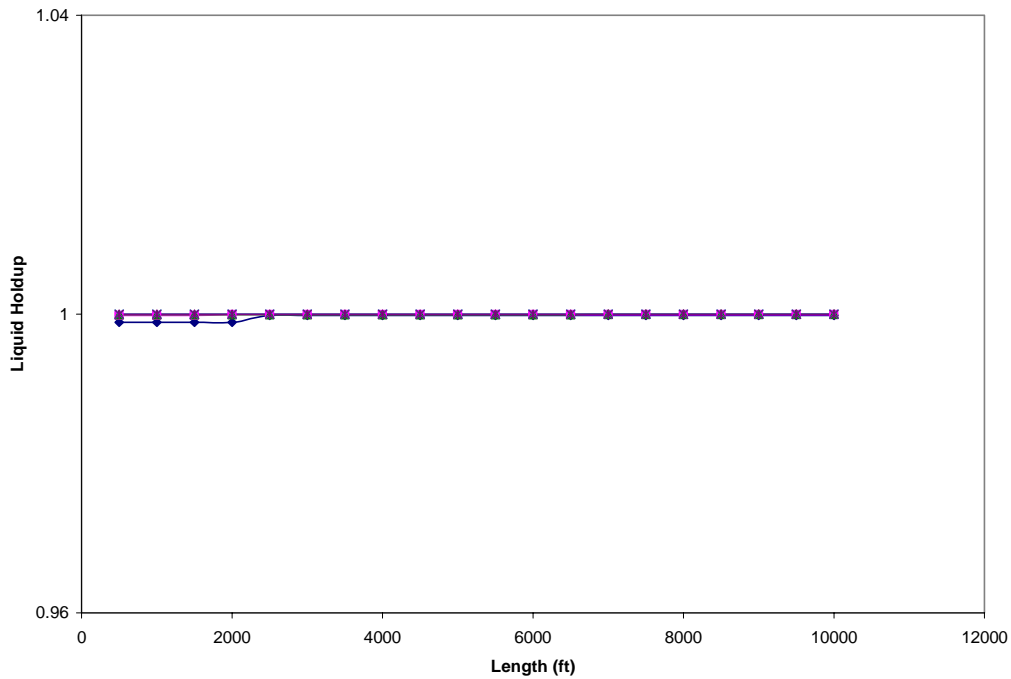


Figure 4-20 Variation of liquid holdup with pipe length for various reservoir temperatures

The plot above, (Figure 4-20) shows the relationship between liquid holdup, length, and temperature. It can be seen that there is no significant change in the values of holdup along the pipe length for the various temperature values.

Effect of Gas-Oil Ratio

Various GORs were used to calculate pressure values for both pipeline and wellbore flow. The GORs used are 750, 1000, 1500, 3000 and 5000, all in scf/bbl. The plot showing the variation of holdup with pipe length at various GORs for horizontal flow is shown in Figure

4-21, while the plot showing the relationship between holdup and pipe length at various GORs for horizontal flow is shown in Figure 4-22.

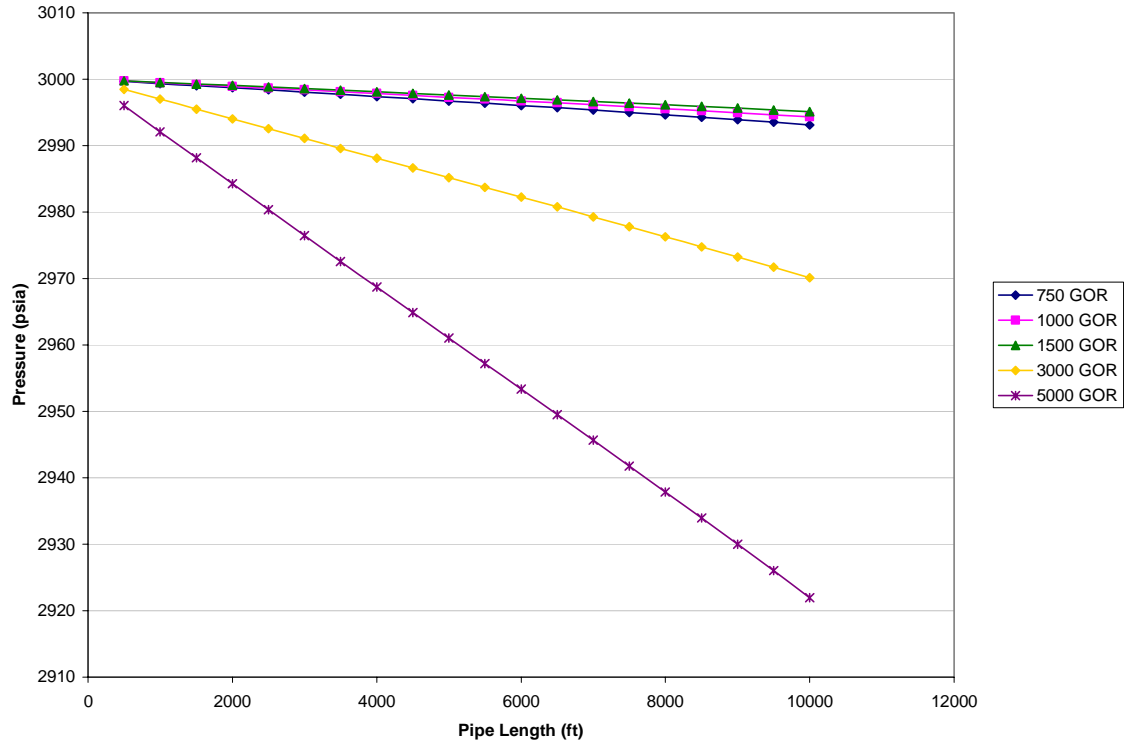


Figure 4-21 Variation of pressure with pipe length at various GORs for horizontal flow

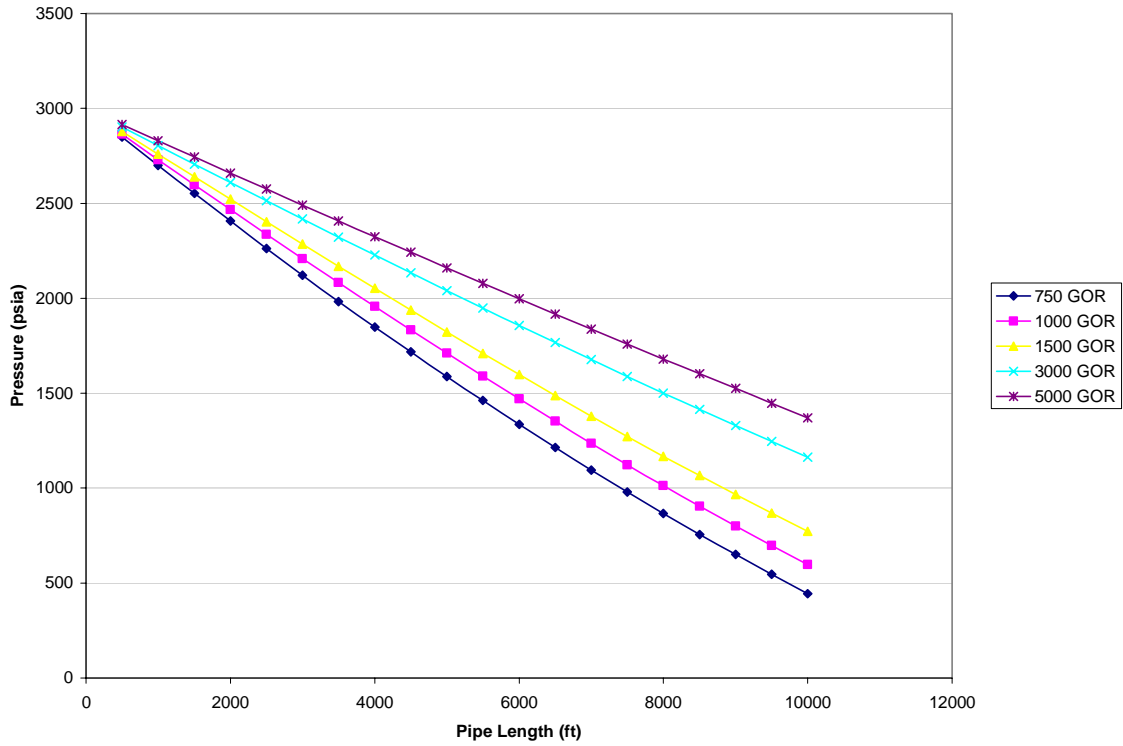


Figure 4-22 Variation of pressure with pipe length at various GORs for vertical flow

For pipeline flow, a decrease in pressure was observed as GOR increased. In the case of wellbore flow, lower GOR values yielded lower pressure values than higher GOR values.

Liquid Holdup and Pressures for Vertical and Horizontal Flow

This study examined the effect of liquid holdup on pressure loss based on pipe orientation from vertical or horizontal.

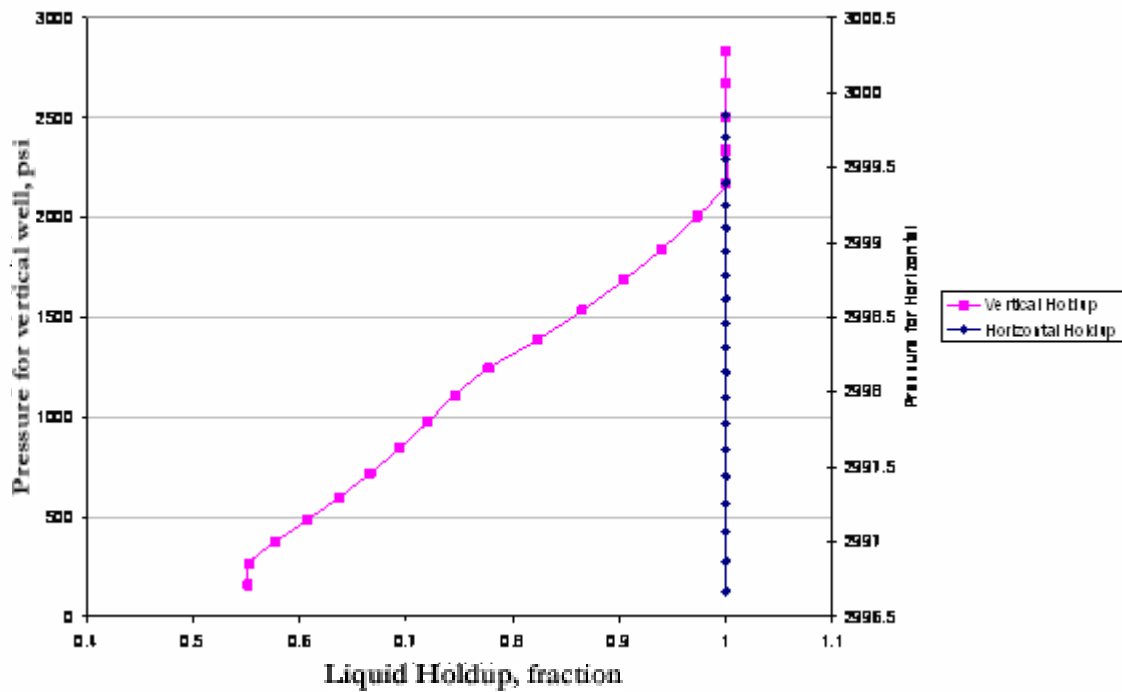


Figure 4-23 Pressure versus Liquid Holdup for Vertical and Horizontal flow

In horizontal flow, holdup remains constant at all pressures. The holdup values in vertical flow starts by being constant, and later reduces as pressure reduces. This is shown in Figure 4-23.

Effect of Pipe Internal Diameter

The software was used to study the effect of pressure loss along the length of the pipe for horizontal (Figure 4-24) and vertical flow (Figure 4-25) based on the internal diameter of the pipe. The following pipe internal diameters (ID) were used: 15.376", 9.95", and 5.46".

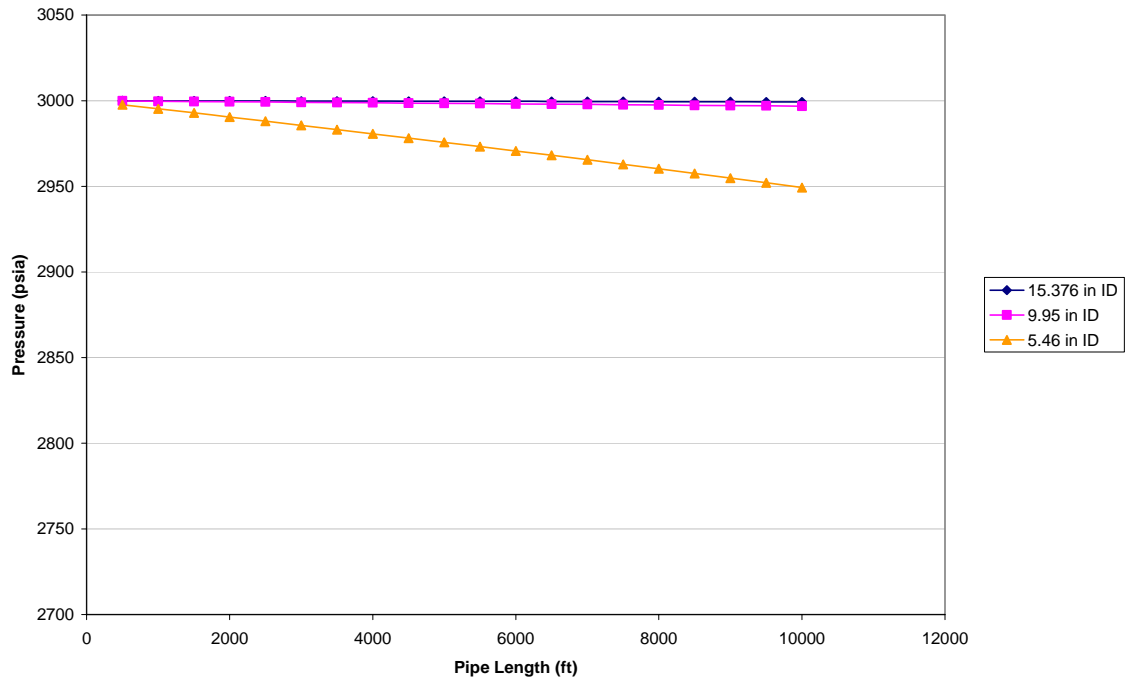


Figure 4-24 Variation of pressure with pipe length for horizontal Flow based on pipe ID

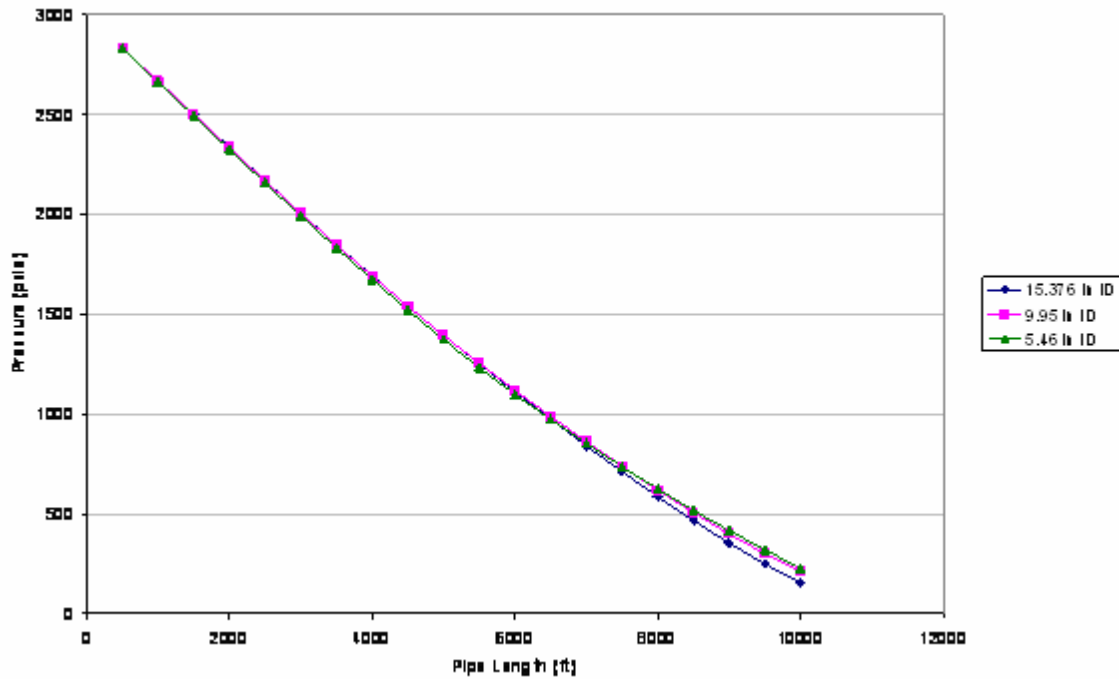


Figure 4-25 Variation of pressure with pipe length for vertical flow based on pipe ID

In pipeline flow, there is little pressure change between the 15.376” and 9.95” pipes. The 5.46” pipe shows more difference pressure. Generally, as pipe ID decreases, pressure in the pipes decrease.

In wellbore flow, the values for pressure change at a faster rate along the length of the pipe. It is also observed that as pipe ID decreases, pressure along the length of the pipe increases.

Effect of pipe ID on heat transfer coefficient

Using the software designed in this study, it was observed that a relationship exists between heat transfer coefficient and the internal diameter of the pipe. The same values of heat transfer coefficient were obtained for both horizontal and vertical flow. This is because the correlations in calculating heat transfer coefficient do not require pipe angle or orientation. This relationship is shown in Figure 4-26 below.

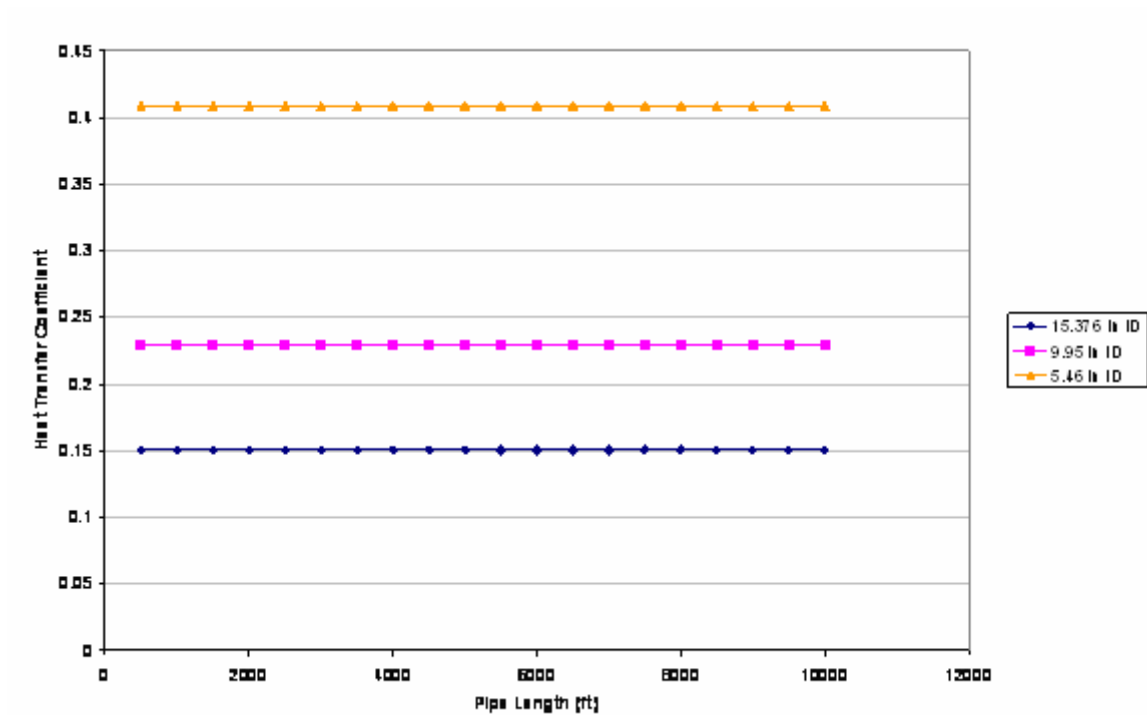


Figure 4-26 Heat Transfer Coefficient for different pipe sizes

It is observed from Figure 4-26 that a smaller pipe will yield a higher heat transfer coefficient. This is because there will be less heat loss in smaller pipes than in larger pipes.

Effect of pipe size on holdup for Vertical Flow

For pipes with a horizontal orientation, the software shows that liquid holdup is constant regardless of pipe diameter. On the other hand, holdup values change with pipe diameter along the length of the pipe for wellbore flow. This relationship is shown in Figure 4-27 below.

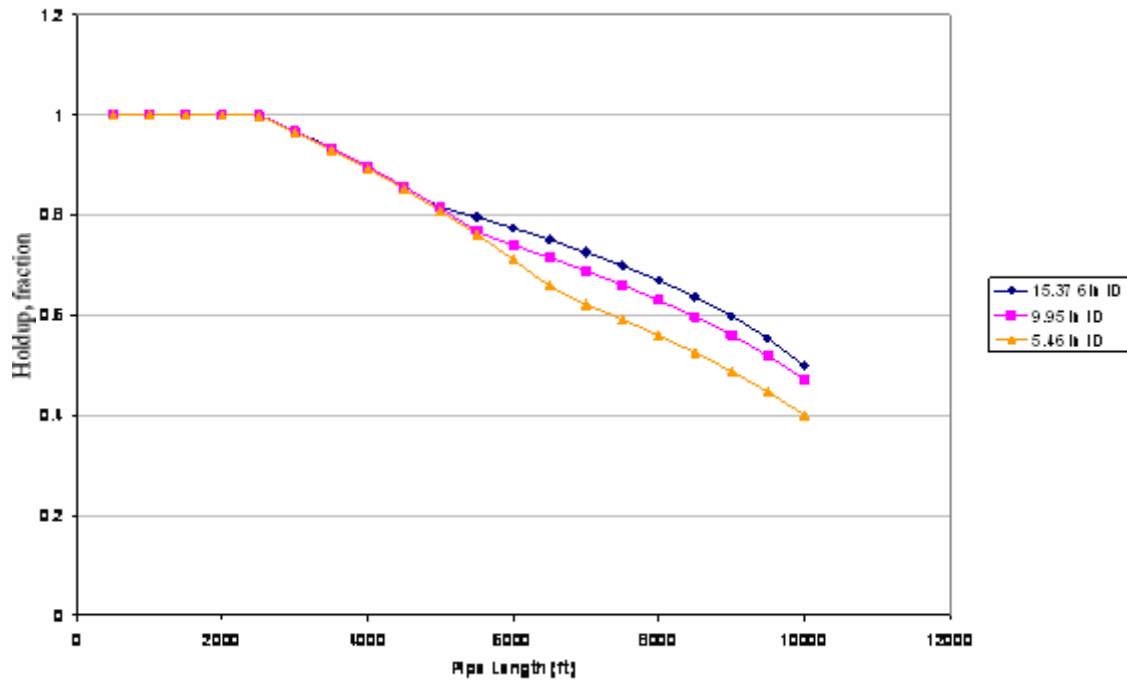


Figure 4-27 Holdup versus Pipe Length Based on Pipe ID for Vertical Flow

Values for liquid holdup start by being equal and constant for all pipe IDs. The values then begin to reduce and remain close for the various pipe sizes. At a certain point along the length of the pipe, holdup values become different for the different pipe IDs. An increase in pipe internal diameter leads to an increase in liquid holdup for vertical flow.

Chapter 5 Conclusions and Recommendations

5.1 Conclusions

Based on this study, the following conclusions are presented:

1. A PC model that analyzes fluid flow and heat transfer was designed.
2. The model provides an insight on the correlations for predicting flow patterns, pressure drops, liquid holdup, and the dependence of thermal transfer on these properties.
3. The software model consists of a prediction model for 2-phase heat transfer that combines 2-phase flow pattern and hydrodynamic models and flow pattern – dependent heat transfer correlations.
4. The software program can be run on any windows based PC, and the results obtained can be exported to a spreadsheet
5. Graphs can be plotted to compare the relationship between the variables.
6. The model was compared with commercial software, Schlumberger's PipeSim, and the results were in agreement.
7. Parameters such as pipe size, pipe orientation (vertical or horizontal), and temperature affect other parameters.
8. The model supports the various conclusions reached by other researchers in the area of fluid flow.

5.2 Recommendations

1. Laboratory experiments should be carried out to determine more effective generalized values for fluid properties as they pertain to heat transfer.
2. These generalized values will be utilized in future models that analyze fluid flow and heat transfer.
3. The effect of flow rate on 2 phase hydrodynamics and thermodynamics can be studied.

References

- Ansari, A. M., Sylvester, N. D., Sarica, C., Shoham, O. and Brill, J. P. (1994). "A Comprehensive Mechanistic Model for Upward Two-Phase Flow in Wellbores". SPE Production & Facilities, May: 143-152.
- Barnea, D. (1986). "A unified model for Predicting Flow-Pattern Transitions for the Whole Range of Pipe Inclinations," Int. J. Multiphase Flow, 12(5): 733-744.
- Beggs, H. D., and Brill, J.P., (1973) "A Study of Two-Phase Flow in Inclined Pipes," Journal of Petroleum Technology, 607-617.
- Brill, J. P. and Mukherjee, H. (1999), "Multiphase Flow in Wellbores", Society of Petroleum Engineers (SPE) Publications, Richardson, TX.
- Chen, Y. (2001), Modeling Gas-Liquid Flow in Pipes: Flow Pattern Transitions and Drift Flux Modeling, MS Thesis, Stanford University, California.
- Dranchuk, P. M., Purvis, R. A. , and Robinson, D. B. (1974) "Computer Calculations of Natural Gas Compressibility Factors Using the Standing and Katz Correlation," Institute of Petroleum Technical Series, No. IP 74-008.
- Dukler, A.E. and Hubbard, M.G. (1975), "A Model for Gas-Liquid Slug Flow in Horizontal and near Horizontal Tubes," Ind. Eng. Chem. Fund., vol. 14, p337.
- Duns, H., Jr. and Ros, N.C.J. (1963). "Vertical Flow of Gas and Liquid Mixtures in Wells," Proceedings of the 6th World Petroleum Congress, 451 – 465.

- Ghajar A.J. (2005). Non-Boiling Heat-Transfer in Gas-Liquid Flows in Pipes – A Tutorial,” Oklahoma State University, Stillwater, OK.
- Ghajar, A. J. and Kim, J. (2005). “A Non-Boiling Two-Phase Flow Heat Transfer Correlation for Different Flow Patterns and Pipe Inclination Angles,” Proceedings of the 2005 ASME Summer Heat Transfer Conference, San Francisco, California, July 17-22.
- Gomez, L. E., Shoham, O., Schmidt, Z., Chokshi, R. N. and Northug, T. (2000). “Unified Mechanistic Model for Steady-State Two-Phase Flow: Horizontal to Vertical Upward Flow”. SPE Journal, 5 (3): 339-350.
- Govier, G.W. and Aziz, K. (1977). “The flow of complex mixtures in pipes”, R.E.Kreiger Pub. Co., Huntington, New York.
- Kaminsky, R.D. (1999), “Estimation of Two-Phase Flow Heat Transfer in Pipes,” Journal of Energy Resources Technology, Trans. ASME, vol. 121, no. 2, pp. 75-80.
- Kaya, A. S., Chen, X. T., Sarica, C. and Brill, J. P. (1999). “Investigation of Transition from Annular to Intermittent Flow in Pipes”. Proceedings of the 1999 ASME Energy Sources Technology Conference. Houston, TX, February 1-3.
- Kim, D., Ghajar, A.J., Dougherty, R.L., and Ryali, V.K. (1999), “Comparison of 20 Two-Phase Heat Transfer Correlations with Seven Sets of Experimental Data, Including Flow Pattern and Tube Inclination Effects,” Heat Transfer Engineering, vol. 20, no. 1, pp. 15–40.
- Lasater, J.A. (1958). “Bubblepoint Pressure Correlation,” Trans. AIME 213, 379.

Lee, A.L. Gonzalez, M.H., and Eakin, B.E. (1996). "The viscosity on Natural Gases," Journal of Petroleum Technology, Aug. pp. 997-1000.

Manabe, R., Wang, Q., Zhang, H., Sarica, C., and Brill, J. P. (2003). "A Mechanistic Heat Transfer Model for Vertical Two-Phase Flow," SPE 84226. SPE ATCE, Denver, CO, October 5-8.

Mandhane, J. M., Gregory, G. A. and Aziz, K. (1974). "A Flow Pattern Map for Gas-Liquid Flow in Horizontal Pipes". Int. J. Multiphase Flow, 1: 537-553.

Mukherjee, H. and Brill, J.P. (1985). Pressure drop correlations for inclined two-phase flow. Journal Energy Resources Technology. 1, pp. 1003 - 1008.

Orkiszewski, J. (1967). Predicting two-phase pressure drops in vertical pipes. SPE Journal Petroleum Technology 3, pp. 829 - 838.

Petalas, N. and Aziz, K. (1998) "A Mechanistic Model for Multiphase Flow in Pipes". CIM 98-39, Proceedings, 49th Annual Technical Meeting of the Petroleum Society of the CIM, Calgary, Alberta, Canada, June 8-10.

Schlumberger (2003), "Flow Correlations for PipeSim – Manual."

Shah, R. K. and London, A. L. (1978) "Laminar Flow: Forced Convection in Ducts". Academic Press, New York.

Standing, M.B. (1981), "Volumetric and Phase Behavior of Oilfield Hydrocarbon Systems," SPE, Richardson, TX.

Standing, M.B. and Katz, D.L., "Density of Natural Gases," Trans. AIME (1942) 146, 140.

Taitel Y.M. and Dukler, A.E. (1976), "A Model for Predicting Flow Regime Transitions in Horizontal and near Horizontal Gas-Liquid Flow," AlChE Journal, vol. 22, p.47.

Vallejo-Arrieta, V. G. (2002). "Analytical Model to Control Off - Bottom Blowouts Utilizing the Concept of Simultaneous Dynamic Seal and Bullheading", Doctoral Dissertation, Louisiana State University, Louisiana.

Vasquez, M. and Beggs, H.D. (1980). "Correlations for Fluid Physical Property Prediction," Journal of Petroleum Technology, pp.968-970.

Wang, Q., Zhang, H., Sarica, C., and Brill, J. P. (2004) "Unified Model of Heat Transfer in Gas-Liquid Pipe Flow," SPE 90459. SPE ATCE, Houston, TX, October 5-8.

Xiao, J. J., Shoham, O. and Brill, J. P. (1990) "A Comprehensive Mechanistic Model for Two-Phase Flow in Pipelines". SPE 20631, SPE Annual Technical Conference and Exhibition, New Orleans, LA, September 23-25.

Appendix

A. Nomenclature

A = Cross sectional area of pipe

c = specific heat, Btu/lbm-°F

C = Input volume fraction

d_{id} = Pipe internal diameter

d_{od} = Pipe outer diameter

f = Friction factor

f_{wG} = Gas/wall friction factor

f_{wL} = Liquid/wall friction factor

g = Gravitational acceleration

h = heat transfer coefficient, Btu/hr-ft²-°F

h_L = Liquid height

H = Holdup

L = length of pipe, ft

N_{Fr} = Froude number

N_{Nu} = Nusselt number

N_{Pr} = Prandtl number

N_{Re} = Reynolds number

p = Pressure

Q = Volumetric flow rate

S = Pipe perimeter

T = temperature

v_G = Actual gas velocity

v_L = Actual liquid velocity

v_{sG} = Superficial gas velocity

v_{sL} = Superficial liquid velocity

v_m = Volumetric flux of the mixture

Greek Letters

ϵ = Pipe roughness

θ = Pipe inclination angle

μ = Dynamic fluid viscosity

ρ = Fluid density

σ = Interfacial tension/surface tension

τ_i = Interfacial friction shear stress

τ_{wG} = Gas/wall friction shear stress

τ_{wL} = Liquid/wall friction shear stress

Subscripts

B = bulk

G = Gas phase

i = Interfacial

L = Liquid phase

O = outside (surrounding)

tp = two-phase

B. Basic Oil and Gas Properties

The estimation of fluid physical properties can be determined by the use of correlations based on pressure-volume-temperature (PVT) parameters. These correlations are important in the application of 2-phase oil-gas flow. Most of these correlations are empirical in nature and are based on a limited quantity of representative samples of data (Mukherjee and Brill, 1999). The restrictions are as a result of the fact that some of the PVT parameters are obtained from samples of reservoir fluids from particular geographic regions that and might not work correctly if applied to other locations where the fluid samples are different. The physical properties of reservoir fluids are pressure and temperature dependent.

B.1 Gas Properties

This section deals with the PVT properties of reservoir gas, such as pseudocritical temperature (T_c) and pressure (p_c), gas deviation factor (z), gas formation volume factor (B_g), gas viscosity (μ_g), and gas isothermal compressibility (c_g).

B.1.1 Pseudocritical and Pseudoreduced Properties

A set of empirical equations was developed by Standing (1981) to determine the pseudocritical temperature and pressure.

Natural Gas Systems

$$T_{pc} = 168 + 325\gamma_g - 12.5\gamma_g^2 \quad (\text{B.1})$$

$$p_{pc} = 677 + 15.0\gamma_g - 37.5\gamma_g^2 \quad (\text{B.2})$$

Gas Condensate Systems

$$T_{pc} = 187 + 330\gamma_g - 71.5\gamma_g^2 \quad (\text{B.3})$$

$$p_{pc} = 706 + 51.7\gamma_g - 11.1\gamma_g^2 \quad (\text{B.4})$$

Where γ_g is the Gas Gravity.

If gas composition is available, the gas gravity and pseudocritical properties is determined from the composition rather than the empirical correlations. This is a more accurate approach. Natural gas consists of multiple gaseous components such as methane, carbon dioxide, propane etc, and each component is a certain percentage in the total mixture. The table below shows the properties of various components.

Constituent, i	Symbol	γ_{gi}	$T_{ci}, ^\circ\text{R}$	p_{ci}, psia
Nitrogen	N ₂	0.9672	227.3	493
Carbon Dioxide	CO ₂	1.5195	547.6	1071
Hydrogen Sulfide	H ₂ S	1.1765	672.4	1306
Methane	CH ₄	0.5539	343.04	667.8
Ethane	C ₂ H ₆	1.0382	549.76	707.8
Propane	C ₃ H ₈	1.5225	665.68	616.3
Isobutane	C ₄ H ₁₀	2.0068	734.65	529.1
N-Butane	n-C ₄ H ₁₀	2.0068	765.32	550.7
iso-Pentane	C ₅ H ₁₂	2.4911	828.77	490.4
N-Pentane	n-C ₅ H ₁₂	2.4911	845.4	486.6
N-Hexane	n-C ₆ H ₁₄	2.9753	913.4	436.9
N-Heptane	n-C ₇ H ₁₆	3.4596	972.5	396.8
N-Octane	n-C ₈ H ₁₈	3.9439	1023.89	360.6
N-Nonane	n-C ₉ H ₂₀	4.4282	1070.35	332
N-Decane	n-C ₁₀ H ₂₂	4.9125	1111.8	304
Oxygen	O ₂	1.1048	278.6	736.9
Hydrogen	H ₂	0.0696	59.9	188.1
Helium	He	0.138	9.5	33.2
Water	H ₂ O	0.622	1165.3	3208

Table B-1 Properties of various natural gas components

The following equations are used to compute the physical properties of natural gas using gas composition:

$$\gamma_g = \sum_{i=1}^n \gamma_{gi} (y_i) \quad (\text{B.5})$$

$$T_{pc} = \sum_{i=1}^n T_{ci} (y_i) \quad (\text{B.6})$$

$$P_{pc} = \sum_{i=1}^n P_{ci} (y_i) \quad (\text{B.7})$$

where y_i = mole fraction of the i th component

and γ_{gi} = gravity of the i th component

T_{ci} = critical temperature of the i th component

p_{ci} = critical pressure of the i th component

The pseudoreduced properties (T_{pr} and p_{pr}) are related to the pseudocritical properties by the following equations:

$$T_{pr} = \frac{T_R + 460}{T_{pc}} \quad (\text{B.8})$$

$$p_{pr} = \frac{p_R}{p_{pc}} \quad (\text{B.9})$$

B.1.2 Gas Deviation Factor (z-factor)

The gas deviation is obtained from the pseudoreduced properties. It is a measure of the deviation of natural gases from the behavior of ideal gases at reservoir conditions. A deviation of 1 for natural gas means that it behaves like an ideal gas. The Dranchuk, Purvis and Robinson correlation (1974) is used because of the ease of utilizing it in a computer program. It is an 11 constant empirical equation used to fit z-factor curves (Mukherjee and Brill, 1999) such as that of Standing and Katz (1942).

$$z = \frac{0.27 p_r}{\rho_r T_r} \quad (\text{B.10})$$

The pseudoreduced density, ρ_r , is found iteratively using the Newton-Raphson iteration.

$$f(\rho_r) = A\rho_r^6 + B\rho_r^3 + C\rho_r^2 + D\rho_r + E\rho_r^3(1 + F\rho_r^2)e^{(-F\rho_r^2)} - G \quad (\text{B.11})$$

$$f'(\rho_r) = 6A\rho_r^5 + 3B\rho_r^2 + 2C\rho_r + D + E\rho_r^2[3 + F\rho_r^2(3 - F\rho_r^2)]e^{(-F\rho_r^2)} \quad (\text{B.12})$$

$$\rho_{r+1} = \rho_r - \frac{f(\rho_r)}{f'(\rho_r)} \quad (\text{B.13})$$

$$A = 0.06423$$

$$B = 0.5353T_r - 0.6123$$

$$C = 0.3151 T_r - 1.0467 - (0.5783/T_r)$$

$$D = T_r$$

$$E = 0.0.6816/T_r$$

$$F = 0.6845$$

$$G = 0.27(Q_c)$$

$$\rho_r = \frac{0.27 p_r}{z T_r}$$

Range of validity:

$$1.05 \leq T_r \leq 3.0$$

$$0 \leq p_r \leq 30$$

B.1.3 Gas Formation Volume factor

The gas formation volume factor, B_g , is the ratio of the gas volume at reservoir conditions and gas volume at standard conditions. It is used to convert surface measured volumes to reservoir conditions. B_g is expressed in SCF/cu.ft (or its inverse – cu.ft/SCF) or SCF/barrel.

$$B_g \left(SCF/ft^3 \right) = \frac{T_{sc} p_R}{p_{sc} z T_R} \quad (B.14)$$

$$B_g \left(ft^3/SCF \right) = \frac{p_{sc} z T_R}{T_{sc} p_R} \quad (B.15)$$

where T_{sc} = standard temperature in °R

p_{sc} = standard pressure (atmospheric) in psia

T_R = reservoir temperature in °F

p_R = reservoir pressure in psia

B.1.4 Gas Viscosity

Gas viscosity, μ_g , is the ratio of the shear stress to the shear rate. The common unit used is centipoises.

$$\mu_g = Ae^{(B\rho^C)} \quad (\text{B.16})$$

$$A = \frac{(9.40 + 0.02M_g) + (T_R + 460)^{1.5}}{[209 + 19M_g + (T_R + 460)]10^4} \quad (\text{B.17})$$

$$B = 3.5 + \frac{986}{(T_R + 460)} + 0.01M_g \quad (\text{B.18})$$

$$C = 2.4 - 0.2B \quad (\text{B.19})$$

$$\rho' = \frac{p_R M_g}{zR(T_R + 460)} \quad (\text{B.20})$$

$$\text{Molecular weight, } M_g = 28.97\gamma_g \quad (\text{B.21})$$

B.1.5 Gas Isothermal Compressibility

Gas isothermal compressibility, c_g , is the change in volume per unit volume of gas for a unit change in pressure (1958). Lee et al (1996) provided a correlative formula that has the same coefficients (A, B, C, D, E and F) as those in the work of Dranchuk et al (1974).

$$c_g = \frac{c_r}{p_c} \quad (\text{B.22})$$

$$c_r = \frac{1}{p_r \left[1 + \left(\frac{\rho_r}{z} \right) \left(\frac{\partial z}{\partial \rho_r} \right) \right]} \quad (\text{B.23})$$

$$\frac{\partial z}{\partial \rho_r} = \frac{1}{\rho_r T_r} \left[5A\rho_r^5 + 2B\rho_r^2 + C\rho_r + 2E\rho_r (1 + F\rho_r^2 - F^2\rho_r^4) e^{(-F\rho_r^2)} \right] \quad (\text{B.24})$$

B.2 Oil Properties

This section deals with the estimation of oil PVT properties from empirical correlations. Properties used here include oil gravity ($^{\circ}API$), oil viscosity, oil formation volume factor, bubblepoint pressure etc.

B.2.1 Specific Property of Oil

The gravity of crude is reported in $^{\circ}API$, and it ranges from 8 $^{\circ}API$ to 58 $^{\circ}API$. Lighter crude oils have higher $^{\circ}API$ values than heavier crudes. The relationship between API gravity and specific gravity of crude oil is shown in the equations:

$$\gamma_o = \frac{141.5}{131.5 + ^{\circ}API} \quad (B.25)$$

$$^{\circ}API = \frac{141.5}{\gamma_o} - 131.5 \quad (B.26)$$

B.2.2 Bubblepoint Pressure

Bubblepoint is the point at which an infinitesimal quantity of gas is in equilibrium with a large quantity of fluid (Standing, 1981). It is the pressure at which the first gas comes out of solution in oil. Hence, when the pressure is above bubblepoint, the fluid is capable of holding additional gases or liquids at the existing pressure and temperature.

$$p_b = 18.2 \left[\left(\frac{R_s}{\gamma_g} \right)^{0.83} \times 10^{[0.00091(T_R) - 0.0125(^{\circ}API)]} - 1.4 \right] \quad (B.27)$$

R_s is the produced oil-gas ratio (SCF/STB)

T_R is the reservoir temperature in °F.

B.2.3 Oil Viscosity

This is an indication of the resistance of oil to flow.

Dead Oil

$$\mu_{Od} = 10^A - 1 \quad (\text{B.29})$$

$$\text{where } A = BT_R^{-1.163} \quad (\text{B.30})$$

$$B = 10^C \quad (\text{B.31})$$

$$C = 3.0324 - 0.02023(^{\circ}API) \quad (\text{B.32})$$

Range of validity: $16 < ^{\circ}API < 58$

$$70 < T_R < 295^{\circ}F$$

Live Oil (above bubblepoint pressure)

$$\mu_O = \mu_{Obp} \left[\frac{P_R}{(P_{bp})^A} \right] \quad (\text{B.33})$$

$$\text{where } A = 2.6P_R^{1.187} e^{[-8.98(10^{-5})P_R - 11.513]} \quad (\text{B.34})$$

Range of validity: $15.3 < ^{\circ}API < 59.5$

$$0.511 < \gamma_g < 1.351$$

$$111 < p_R < 9485 \text{ psi}$$

Live Oil (below bubblepoint pressure)

$$\mu_{Ob} = A(\mu_{Od})^B \quad (\text{B.35})$$

where $A = 10.715(R_{sb} + 100)^{-0.515}$ (B.36)

$$B = 5.44(R_{sb} + 150)^{-0.338} \quad (\text{B.37})$$

Range of validity: $16 < \text{°API} < 58$

$$20 < R_{sb} < 2070 \text{ SCF} / \text{ bbl}$$

$$70 < T_R < 295 \text{ °F}$$

$$14.7 < p_R < 5265 \text{ psi}$$

At bubblepoint pressure

$$\mu_{Obp} = \mu_{Ob} \text{ at } R_{sb} = R_{si} \quad (\text{B.38})$$

The range of validity is the same as that below the bubblepoint pressure.